Autogenous cross-regulation of *Quaking* mRNA processing and translation balances *Quaking* functions in splicing and translation

W. Samuel Fagg and Manuel Ares, Jr.[1]

Center for Molecular Biology of RNA

Department of Molecular, Cell & Developmental Biology

Sinsheimer Laboratories

UC Santa Cruz. Santa Cruz, CA 95064

[1]Corresponding author. Email ares@ucsc.edu Phone (831) 459-4628

Running Head: Autoregulatory control of Qk protein isoforms

Keywords: Quaking, Qk, QKI, RNA binding protein, autoregulation, RNA processing

Abstract

Quaking RNA binding protein (RBP) isoforms arise from a single *Quaking* gene, and bind the same RNA motif to regulate splicing, stability, decay, and localization of a large set of RNAs. However, the mechanisms by which the expression of this single gene is controlled to distribute appropriate amounts of each *Quaking* isoform to regulate such disparate gene expression processes are unknown. Here we explore the separate mechanisms that regulate expression of two isoforms, Quaking-5 (Qk5) and Quaking-6 (Qk6), in mouse muscle cells. We first demonstrate that Qk5 and Qk6 proteins have distinct functions in splicing and translation respectively, enforced primarily through differential subcellular localization. Using isoform-specific depletion, we find both Qk5 and Qk6 act through *cis* and *trans* post-transcriptional regulatory mechanisms on their own and each other's transcripts, creating a network of auto- and cross-regulatory controls. Qk5 has a major role in nuclear RNA stability and splicing, whereas Qk6 acts through translational regulation. In different cell types the cross-regulatory influences discovered here generate a spectrum of Qk5/Qk6 ratios subject to additional cell type and developmental controls. These unexpectedly complex feedback loops underscore the importance of the balance of Qk isoforms, especially where they are key regulators of development and cancer.

Introduction

Sequence-specific RNA-binding proteins (RBPs) regulate nearly every post-transcriptional step of gene expression. Control is exerted by recognition of cis-acting regulatory sequences by the RNA-binding domain (RBD), followed by one or more consequences, including restructuring of the RNA and the protein, altered interactions with other proteins, and the generation of activities that influence the function of RNA polymerase, the spliceosome, the export and decay machinery, and the ribosome (Keene 2007; Fu and Ares 2014). Furthermore, many RBPs control their own levels (autogenous regulation), through the same mechanisms by which they regulate their targets (Wollerton et al. 2004; Lareau et al. 2007; Ni et al. 2007; Damianov and Black 2010; Sun et al. 2010). In many metazoans, multiple RBPs with the same or highly similar RBDs (iso-specific) perform distinct functions but are expressed at the same time in the same cells (Makeyev et al. 2007; Spellman et al. 2007; Yeo et al. 2009; Gehman et al. 2011; Charizanis et al. 2012; Gehman et al. 2012; Singh et al. 2014), suggesting that any functional diversification must be enforced by regulatory mechanisms that prevent crosstalk. These two circumstances, autogenous regulation through binding their own pre-mRNAs and mRNAs, combined with functional diversification using the same RBDs and recognition sequences create a regulatory conundrum: How is the right amount of each distinctly functional iso-specific RBP isoform in a cell established and maintained?

Since all isoforms within a family recognize essentially the same RNA sequence, isoform-specific control is unlikely to be mediated through recognition of distinct cis-acting RNA sequences. Two other mechanisms include 1) isoform-specific localization

that restricts function to processes within specific compartments (Caceres et al. 1998; Koizumi et al. 1999; Cazalla et al. 2002; Sanford et al. 2004), and 2) interactions between a specific RBP family member and specific elements of a target core machinery (Roscigno and Garcia-Blanco 1995; Jin et al. 2004; Cheever and Ceman 2009; Sharma et al. 2011) mediated by isoform-specific amino acids. Because many RBPs are encoded by multi-gene families with complex alternative splicing (Underwood et al. 2005), whole menageries of functionally distinct RBP isoforms that recognize the same RNA target can be expressed within single cell types (Lee et al. 2009; Hamada et al. 2013; Lee et al. 2016). How does the cell recognize when each distinctly functional RBP family member is present in an appropriate amount for each process?

To examine this question, we have focused on the single *Quaking* gene (*QKI* in human, *Qk* in mouse), which is required for a broad set of functions in diverse tissues (Ebersole et al. 1996; Darbelli et al. 2016), through its contribution to RNA processing steps including splicing (Hall et al. 2013; van der Veer et al. 2013; Darbelli et al. 2016), localization (Li et al. 2000; Larocque et al. 2002), stability/decay (Li et al. 2000; Larocque et al. 2005; Zearfoss et al. 2011; de Bruin et al. 2016a), translation (Saccomanno L 1999; Zhao et al. 2010), and miRNA processing (Wang et al. 2013; Zong et al. 2014). These processes are regulated by dimeric Qk binding an RNA element that includes ACUAAY and a “half-site” (UAAY) separated by at least one nucleotide (Ryder and Williamson 2004; Galarneau and Richard 2005; Beuck et al. 2012; Teplova et al. 2013). *Quaking* transcription initiates primarily at a single major site, and in most cell types, three alternatively spliced mRNAs encode three protein isoforms [Quaking-5 (Qk5), Quaking-6 (Qk6), and Quaking-7 (Qk7)] that differ only in the C-terminal tail

(Ebersole et al. 1996; Kondo et al. 1999). Although various cell types express different ratios of Qk protein isoforms (Ebersole et al. 1996; Hardy et al. 1996; Hardy 1998; van der Veer et al. 2013; de Bruin et al. 2016a), it is unclear how the relative isoform ratios are maintained in order to support tissue-specific regulated RNA processing but disruption of these ratios leads to developmental defects (Ebersole et al. 1996; Cox et al. 1999), cancer (Sebestyen et al. 2015; de Miguel et al. 2016), and schizophrenia (Aberg et al. 2006).

Many studies of Quaking function have used overexpression of Qk isoforms (Wu et al. 2002; Wang et al. 2013), or depletion strategies or mutant models that do not distinguish which Qk isoform is functional (Hardy et al. 1996; Lu et al. 2003; van der Veer et al. 2013). Here we test specific Qk isoforms for separate functions, and identify in part how the appropriate balance of Qk isoforms is maintained. In mouse myoblasts, Qk5 and Qk6 are the predominantly expressed isoforms and we find that Qk5, but not Qk6, regulates splicing, while Qk6 controls mRNA translation and decay. This functional specificity is mediated by subcellular localization encoded into the unique C-terminal amino acids of these isoforms. Furthermore, the relative expression of Qk protein isoforms is regulated in part, by Qk protein isoforms themselves through both auto- and cross-regulatory influences characteristic of the function of each isoform on its other RNA targets. These findings uncover unexpectedly complex isoform control within a single family of RBPs, and suggest that the relative amounts of each isoform are set in a cell type specific fashion and homeostatically controlled by Qk protein isoform levels themselves.

Results

Qk5 and Qk6 are the predominant isoforms in myoblasts

We analyzed the abundance and localization of Qk isoforms (Fig 1A) in myoblasts and differentiated myotubes (Yaffe and Saxel 1977) using isoform-specific antibodies. Total Qk protein level increases during C2C12 myoblast differentiation ((Hall et al. 2013), Fig 1B), with Qk5 the most abundant, followed by Qk6, and then Qk7, which is barely detectable (Fig 1B). Differentiation leads to myotube fusion ((Yaffe and Saxel 1977) Fig 1C), and each isoform increases proportionately (Fig 1B). Consistent with previous studies in glia (Hardy et al. 1996; Lu et al. 2003), in myoblasts and myotubes Qk5 is primarily nuclear, although some cytoplasmic localization is observed (Fig 1D). In contrast, Qk6 and Qk7 are primarily cytoplasmic, but can be detected in both nuclear and cytoplasmic compartments, with noticeable cell-to-cell heterogeneity (Fig 1D). We conclude that Qk5 and Qk6 are the major Qk isoforms in C2C12 myoblasts, and their overall subcellular localization is similar (although not identical) to that observed in glia.

Qk-dependent alternative splicing regulation requires Qk5, but not Qk6

We previously showed that depletion of all Qk isoforms alters splicing of several hundreds of exons in myoblasts, and that one or more unknown Qk isoform(s) directly promotes inclusion of Capzb exon 9 by binding to downstream intronic ACUAA sequence elements (Hall et al. 2013). Since Qk5 is the most abundant and primarily nuclear Qk isoform in myoblasts, we tested the hypothesis that Qk5 is responsible for splicing regulation. We overexpressed a Myc-tagged cDNA construct for each isoform

(Fig S1A), and tested the effect on splicing of the Qk-regulated Capzb exon 9 in the β–globin reporter (pDUP51, Dominski and Kole 1991), which includes ~200 nucleotides upstream and ~250 nucleotides downstream of Capzb exon 9 (Dominski and Kole 1991; Hall et al. 2013). To our surprise, overexpression of either predominantly nuclear Myc-Qk5 or nuclear and cytoplasmic Myc-Qk6 (Fig 1E) efficiently activates splicing (Fig 1F).

Previous work has shown that Qk proteins are only stable as a dimer *in vivo* (Beuck et al. 2012), and that overexpression of Qk isoforms can create ectopic Qk heterodimers (Pilotte et al. 2001). Given this, we hypothesized that overexpression of Myc-Qk6 could drive formation of dimers with Qk5, leading to aberrant Myc-Qk6 nuclear import as part of a Myc-Qk6-Qk5 heterodimer (Pilotte et al. 2001), which could activate exon inclusion. Consistent with this, we observe strong nuclear staining of Myc-Qk6, which appears throughout cells that overexpress it (Fig 1E). To rigorously test Qk6 function in splicing, we used a depletion-replacement strategy in which all endogenous Qk mRNAs were depeleted using an siRNA to a common region, followed by expression of a single isoform carrying translationally silent siRNA resistant mutations (kind gift from Sean Ryder) to create a cellular pool of Qk dominated by a single isoform (Fig S1B). Under the depletion-replacement treatment, inclusion of Capzb reporter exon is specifically increased by replacement with Myc-Qk5, but not with Myc-Qk6 (Fig 2A and 2B). In addition, whereas Myc-Qk5 accumulates efficiently in the nucleus, Myc-Qk6 remains primarily cytoplasmic (Fig 2C). Taken together, we conclude that Qk5 is predominantly nuclear and serves as a splicing factor, but Qk6 is not, suggesting that this isoform regulates translation (Saccomanno L 1999) in myoblasts also and typically does not directly contribute to splicing regulation.

Nuclear presence of the common Qk protein sequence is sufficient for splicing function

The observation that overexpression and nuclear accumulation of Myc-Qk6 activates splicing inappropriately (compare Fig 1E and 1F to 2B and 2C) suggests that nuclear localization of the common (ie non-isoform specific) parts of Qk might be sufficient to activate splicing. The C-terminal 30 amino acids of Qk5 encode a non-canonical NLS (Wu et al. 1999), however other function(s) specifically necessary for splicing could also be contained in this region. To test this, we made two Qk constructs lacking any isoform-specific C-terminal amino acids (i.e., only the common or "body" 311 amino acids shared by all natural Qk isoforms, Fig 1A). One construct encoded an N-terminal HA epitope tag (HA-QkBody), and the other an N-terminal HA tag followed by the canonical SV40 NLS (HA-NLS-QkBody, Fig 2D). Upon expression in myoblasts (Fig S2), these mutant Qk proteins promote inclusion of Capzb exon 9, whether endogenous Qk protein is depleted or not (Fig 2E). This shows that all necessary residues required for Qk splicing functions reside in the body of the Qk protein and not in the Qk5 isoform-specific tail. The HA-QkBody protein is distributed throughout the cell, whereas the HA-NLS-QkBody protein is concentrated in nuclei (Fig 2F), reinforcing the conclusion that nuclear localization of the common regions of the Qk protein is sufficient for splicing function. Furthermore, it is the compartmentalization in the nucleus mediated by the Qk5-specific tail that determines the fate of Qk5 as a splicing factor. The isoform specific tail of Qk6 contributes to its concentration in the cytoplasm and greatly limits its contributions to splicing as compared to the QkBody mutant protein that is localized in both the nucleus and cytoplasm (compare Figs 2C and 2F).

Qk5 is required for expression of Qk6 and Qk7 at the level of RNA accumulation

To refine the understanding of Qk isoform-specific functions obtained from cells expressing single Qk protein isoforms, we selectively targeted individual protein isoforms using isoform-specific siRNAs (siQk5 or siQk6/7; see Fig 3A). Treatment with siQk5, but not siQk6/7 produces the expected alternative splicing changes (Hall et al. 2013) in the endogenous Rai14 cassette exon 11 (loss of repression, Fig 3B) and the Capzb exon 9 splicing reporter (loss of activation, Fig 3C). However, treatment with siQk5 also leads to the unexpected loss of all Qk protein isoforms (Fig 3D, compare to treatment with pan-Qk siRNA), whereas treatment with siQk6/7 leads only to the loss of Qk6 and 7 (Fig 3D and S3A). We are confident that this is due to specific depletion of the Qk5 mRNA by the Qk5-1 siRNA, because two additional Qk5-specific siRNAs (Fig 3A) lead to the same loss of all Qk RNAs (Fig 3E) and proteins (Fig S3B). Depletion of Qk6 and Qk7 proteins by Qk5-specific siRNA is as efficient as that observed with a Qk6/7-specific siRNA (Fig S3A). We interpret these data to mean that cells cannot express Qk6 or Qk7 RNA or protein unless they also or first express Qk5 protein. We conclude that Qk5 is required to promote efficient accumulation of the major mRNAs produced by the Qk gene.

Qk proteins can bind the Qk6 mRNA 3' UTR (Hafner et al. 2010; Van Nostrand et al. 2016), and phylogenetically conserved Qk sequence motifs are also found in this sequence ((Paz et al. 2014) Fig S3C), however it is unclear whether binding of Qk5 or Qk6, or both occurs at this site, and what the physiological consequences of these binding events might be. To test whether Qk5 contributes to Qk6 protein expression through

binding to the Qk6 3' UTR, we made a reporter gene with the Qk6 3'UTR fused to the renilla luciferase coding region, and co-transfected it with a firefly luciferase control reporter (Fig S3D), and either control (siNT), siQk, or siQk5-1 siRNAs (siQk6/7 was not used in this experiment because it will deplete the Qk6 reporter transcript directly). Treatment with either siQk or siQk5-1 efficiently depletes all Qk protein isoforms (Fig S3D), and we observe no change in reporter protein abundance (Fig S3E). We conclude that Qk proteins are not required for Qk6 3'UTR reporter protein accumulation (Fig S3E). Taken together with Qk5's nuclear localization, and the observation that depletion of Qk5 mRNA results in loss of Qk6/7 mRNA and protein (Figs 3D, 3E, S3A, and S3B), we suggest that Qk5 regulates Qk6 expression by promoting pre-mRNA accumulation, consistent with its function as a splicing factor (Figs 3B and 3C).

Qk nuclear RNA accumulation requires Qk5 protein

To test the idea that Qk5 promotes overall Qk RNA accumulation (Fig 3E), we performed subcellular fractionation of C2C12 cells treated with siNT, siQk5, or siQk6/7. Because siRNA is effective in the cytoplasm (Sen and Blau 2005), we expect that changes in nuclear RNA result directly or indirectly from reduction in Qk protein, rather than from siRNA treatment. Western blots show efficient knockdown of all Qk protein isoforms by siQk5 in both whole cell extracts (WCE) and nuclear fractions (Fig 4A). In the nuclear fractions Histone H3 is abundant, whereas Gapdh is nearly undetectable (Fig 4A, right), indicating the nuclear fractions are free of cytoplasm. To test if Qk5 is required for nuclear transcript accumulation of Qk isoforms, we extracted RNA from the nuclear fractions and measured Qk RNAs, and as a control 7SK RNA. We find that

depletion of Qk5 protein results in significant reduction of both Qk6/7 transcripts, as well as its own transcript in nuclear extracts (Fig 4B). Because this assay measures specific parts of the same pre-mRNA destined for the distinct Qk mRNA isoforms, a simple interpretation is that Qk5 protein is required for stabilization of nuclear Qk pre-mRNA, and that upon loss of this function, all the Qk mRNAs fail to accumulate.

Qk5 promotes accumulation of its own mRNA through splicing

To test whether Qk5 protein promotes accumulation of its own transcript through splicing or polyadenylation, we measured the fraction of Qk5 RNA that remains unspliced upstream of the last isoform-specific 3' splice site, as well as the fraction of Qk5 RNA that reads through the major Qk5 polyadenylation site relative to total nuclear Qk5 (Fig S4A) after depletion of either Qk5 or Qk6/7 protein (Fig 4A). Consistent with a role for Qk5 in splicing of its own mRNA, unspliced nuclear Qk5 pre-mRNA increases 40% relative to total nuclear Qk5 RNA when Qk5 protein is depleted ($p < 0.05$; Fig 4C, left side). No significant change in the fraction of transcripts that read through the Qk5 polyadenylation site is observed under Qk5 or Qk6/7 depletion (Fig 4C, right side), suggesting that Qk5 does not regulate polyadenylation of its own mRNA. As a side note, when Qk6 and Qk7 are depleted, the fraction of unspliced nuclear Qk5 RNA decreases ($p < 0.01$; Fig 4C, left side). This is consistent with observations that Qk6/7 depletion affects other Qk5-regulated splicing events (Capzb exon 9 ($p < 0.05$; Fig 3C) and Rai14 exon 11 (Fig 3B) because Qk6 normally represses Qk5 translation (see below). Examination of the Qk5 terminal intron and coding sequence 3'end indicates Qk protein binding sites (Van Nostrand et al. 2016), some of which overlap with conserved

computationally predicted Qk binding sites ((Paz et al. 2014) Fig S4B). We cloned this region into the β globin splicing reporter pDUP51 ((Dominski and Kole 1991) Fig S4B) to test if Qk5 promotes splicing through this minimal sequence. Depletion of Qk protein with siQk5 (Fig S4C) significantly reduces use of this Qk5 3' splice site compared to Gapdh mRNA (Fig 4D), indicating that Qk5 is required for efficient 3' splice site usage. These results support a hierarchical model whereby inefficient production of initially small amounts of Qk5 promote increased expression of Qk5 mRNA through increased terminal 3' splice site usage, leading to increased Qk5 protein, which then increasingly promotes Qk6 and Qk7 RNA expression.

Qk5 inhibits its own expression by 3'UTR binding

Previous studies of mammalian Qk5 (Larocque et al. 2002) or its homolog fly HowL (Nabel-Rosen et al. 2002) suggest a general role for Qk5 as a repressor of gene expression through binding to 3'UTRs. Qk protein binds the Qk5 3'UTR (Hafner et al. 2010; Van Nostrand et al. 2016) in a region that overlaps with one very high confidence predicted binding site ((Paz et al. 2014) Fig S4D). To test the hypothesis that Qk5 might negatively regulate its expression through binding its 3'UTR (independent of its positively acting role through splicing, Figs 4C and 4D), we cloned the entire Qk5 3'UTR into a renilla luciferase reporter construct and either depleted all Qk proteins (siQk) or Qk6 and Qk7 (siQk6/7, N.B. siQk5 targets the reporter and was not used). Depletion of all Qk protein forms, but not Qk6/7 alone (Fig S4E), leads to a 27% increase in renilla protein expression (Fig S4F; $p = 0.08$). This suggests that Qk5 negatively regulates its

own protein levels specifically, especially considering that this effect is not observed using the Qk6 3'UTR reporter (Fig S3E).

Close examination of the Qk5 3'UTR suggest several putative Qk regulatory binding motifs, but only one region contains three overlapping CLIP peaks (Fig S4D). To test the requirement of this motif for Qk5 3'UTR reporter abundance, we substituted TACTAAC (wild-type) with TGGTACC (mutant; see Fig S4D inset) in an otherwise unchanged renilla Qk5 3'UTR reporter construct and measured reporter protein abundances after transfection in C2C12 myoblasts. We find mutation of the Qk binding element UACUAAC results in an increase in reporter protein expression compared to wild type (Fig S4G; $p = 0.07$), similar to the observation upon depletion of Qk protein (Fig S4F). Together these results suggest that Qk5 binds the UACUAAC element in its own 3'UTR to negatively regulate its expression. Thus, Qk5 protein at low levels promotes additional Qk5 mRNA accumulation through splicing, but at high levels acts by binding its own 3' UTR to limit expression through an unknown mechanism.

Qk6 negatively regulates Qk5 protein expression

If Qk5 protein promotes expression of both its own and Qk6 mRNA, then reciprocal influences may exist whereby Qk6 protein feeds back to control Qk5 levels. We performed quantitative western blotting using the Qk5-specific antibody, and detected a reproducible 26% increase in Qk5 protein levels when Qk6 is depleted (Fig 5A). This increase in Qk5 levels is accompanied by a significant increase in Qk5 activity as detected on alternative splicing events under Qk5 control (e. g. Rai14 exon 11 is more repressed, the Capzb exon 9 splicing reporter is activated ($p < 0.05$), and splicing

efficiency of the terminal Qk5 3' splice site increases ((p < 0.01) Figs 3B, 3C, 4C, and 4D (Hall et al. 2013)). This increase in Qk5 protein level and activity upon loss of Qk6 is accompanied by a consistent but modest reduction in Qk5 mRNA level relative to control (Fig 5B). This opposing relationship between RNA stability and translational efficiency has been previously described (Kawai et al. 2004), and suggests that Qk6 protein binding to the Qk5 mRNA stabilizes the transcript while simultaneously repressing its translation. The decrease in Qk5 RNA, together with the increase in Qk5 protein combine to produce a 37% increase in translational efficiency ((Vasudevan and Steitz 2007); p = 0.27) of Qk5 mRNA when Qk6 is depleted. These data indicate that Qk6 is a translational repressor of Qk5 mRNA, consistent with the function of Qk6 on other mRNAs in other cell types (Saccomanno L 1999; Zhao et al. 2010).

Qk6 positively regulates its own translation

During our initial overexpression experiments with Myc-Qk6 we noticed an increase in levels of endogenous Qk6 (Fig S1A). We repeated the overexpression of Myc-Qk6 in myoblasts and performed quantitative western blotting to measure both ectopic and endogenous Qk6. We observe a 2.5-fold increase in endogenous Qk6 protein (p < 0.05; Fig 5C), without a significant RNA level change, indicating a 2.43-fold increase in translational efficiency (p < 0.05; Fig 5C). No significant change is observed in endogenous Qk6 protein levels (Fig 5C) when Myc-Qk5 is overexpressed (Fig S5A), indicating that the ability of Qk5 to promote Qk6 RNA accumulation (Fig 3E) is saturated by endogenous amounts of Qk5 and cannot be further increased. We conclude

that Qk6 promotes translation of its own mRNA, even as it represses translation of Qk5 mRNA (Fig 5A).

To exclude the hypothesis that ectopic Myc-Qk6 increases the level of endogenous Qk6 protein solely through a posttranslational mechanism such as increased homo-dimerization, we measured luciferase expression from the luciferase-Qk6 3'UTR reporter with and without Myc-Qk6 overexpression (Fig S5B). Consistent with the result described above for endogenous Qk6, overexpression of Myc-Qk6 leads to an increase in renilla protein level compared to control (Fig 5D; $p = 0.1$), suggesting Qk6 mediates this effect in part through direct translational control. Thus, the Qk6 3'UTR contains an autoregulatory element through which Qk6 activates its own translation. Taken together with the data in Figs 3 and 4, these results identify a cross-isoform and autoregulatory network in myoblasts where Qk5 is the most abundant isoform and required for all Qk expression; Qk6 is less abundant but promotes its own translation while inhibiting Qk5 translation. These results expose a novel autoregulatory network that helps explain how the different *Qk* RBP family members are controlled to regulate the functional output from this gene in myoblasts.

Qk protein isoform abundance in different cells and tissues

Qk5 is the predominant Qk isoform present in C2C12 myoblasts (Fig S1A). In contrast, Qk6 and Qk7 are the predominant isoforms in adult mouse brain (Hardy et al. 1996). From the cross-isoform regulatory interactions we identified in C2C12 myoblasts, we hypothesize that in cell types with higher Qk6 and lower Qk5 protein: 1) the requirement of Qk5 for Qk6 RNA accumulation is lessened due to amplified positive

autoregulation by Qk6, and 2) Qk6 more efficiently represses the translation of Qk5 mRNA. To test this, we used quantitative western blotting (Fig S6A) to identify cells in which Qk5 protein abundance is lower and Qk6 protein abundance is higher relative to total Qk protein than observed in C2C12 myoblasts. C2C12 cells have a high Qk5/Qk6 ratio (with Qk7 nearly undetectable; Fig S1A; Fig 6A), and, consistent with previous findings (Hardy et al. 1996), adult mouse optic nerve and cerebellum tissue have a much lower Qk5/Qk6 ratio (Fig 6A). In contrast, rat C6 glioma (Benda et al. 1971) and CG4 oligodendrocyte precursor cells (Louis et al. 1992) have intermediate Qk5/Qk6 ratios, with different amounts of Qk6 or Qk7 (Fig 6A). We chose rat C6 glioma cells as a counter example to mouse C2C12 cells to test whether the autoregulatory controls observed above operate in cells with low Qk5/Qk6 ratios.

Cross isoform Qk regulatory control is conserved in C6 glioma cells

We treated C6 glioma cells with siRNAs to deplete either the Qk5 or Qk6/7 isoforms (these target sequences conserved in mouse and rat). Although overall siRNA-mediated depletion appears less efficient in these cells as compared to C2C12 cells, the loss of Qk6/7 upon depletion of Qk5 is evident, indicating that the hierarchical requirement of Qk5 for expression of Qk6/7 RNA (Fig 6E) and protein (Fig 6D) is conserved. The magnitude of the reduction of Qk6 protein in C6 glioma cells is less than that observed in C2C12 myoblasts (down 42% in C6 cells, 67% in C2C12 cells, Fig 6D compare to Fig S3A), however. We also observe an increase in Qk5 expression under Qk6/7 depletion in C6 glioma cells, indicating that the feedback repression of Qk6 on Qk5 is conserved. However, apparent translational efficiency increases by 2.6-fold in C6

glioma cells ($p < 0.01$) compared to 37% in C2C12 myoblasts ($p = 0.27$) in the absence of Qk6/7. Therefore, due to the higher relative concentration of Qk6 in C6 glioma cells the observed translational repression is more efficient. Taken together, these findings reveal that the *Qk* autogenous regulatory network operates at various settings in different cells (Fig 7A), where the Qk5/Qk6/7 isoform ratio can vary in a stable way, using parallel sets of auto- and cross regulatory control. The existence of multiple different stable settings of the Qk5/Qk6/7 ratio suggests that the *Qk* regulatory network is responsive to the influence of other regulatory proteins and RNAs.

Discussion

We initiated this study to understand how RBP family isoforms that recognize the same RNA sequence in different functional contexts (splicing, RNA transport, translation, decay) are regulated within a single cell so that each of these processes is appropriately supplied with the correct amount of RBP. We chose Qk because all isoforms arise form a single gene, to avoid complexities that exist with other RBP families expressed from multiple genes. In the case of Qk, isoforms are assigned roles by compartment: nuclear functions (splicing, RNA biogenesis) are executed by Qk5, whereas cytoplasmic functions (translational control, mRNA decay) are executed by Qk6. Homeostasis and control of the levels of each isoform is established through a network of auto- and cross regulatory controls whereby Qk5 is required for its own and Qk6 RNA expression from the nucleus, and Qk6 activates its own and represses Qk5 mRNA at the translational level (Figs 7A and 7B). The strength of these controls is tunable such that cells express different ratios of Qk5 and Qk6 in a stable characteristic way.

A division of labor between Qk protein isoforms

We previously identified Qk as a regulator of muscle-specific alternative splicing through binding to intronic ACUAA sequence motifs (Hall et al. 2013). Since the Qk5 isoform contains a NLS (Wu et al. 1999), it seemed natural to expect Qk5 to be responsible for splicing. Indeed, Qk5 is both necessary (Figs 3B and 3C) and sufficient (Fig 2B) for splicing regulation, whereas Qk6 and Qk7 are dispensable (Figs 3B, 3C, and S3A). Although artificially overexpressed Myc-Qk6 can activate splicing (Fig 1F), its nuclear localization (Fig 1E) is likely mediated by heterodimerization with endogenous Qk5 (Pilotte et al. 2001). A mutant Qk protein containing all the common Qk sequences but no isoform-specific C-termini (QkBody) is distributed throughout both the nucleus and cytoplasm of C2C12 myoblasts and suffices for splicing, whereas Qk6 does not (Fig 2). A comparison of the widespread distribution of QkBody protein with the predominantly cytoplasmic distribution of Qk6 indicates that the 8 Qk6-specific C-terminal amino acids encode a cytoplasmic retention or nuclear export signal (Nakielny and Dreyfuss 1999; Cook and Conti 2010). Thus, Qk5 appears assigned to nuclear functions, while Qk6 is responsible for cytoplasmic functions, and these functions are enforced by localization elements that reside within the isoform specific amino acids. This suggests that the Qk protein elements required to interact with the splicing, translation, export and decay machineries lie within the protein sequences common to all Qk isoforms, and that additional dissection of Qk protein sequences will be necessary to map the sites required for function in each of those processes.

We (Fig 1A) and others (van der Veer et al. 2013; de Bruin et al. 2016b) also observe some Qk6 that appears nuclear in untransfected cells, possibly but not necessarily mediated by formation of Qk5-Qk6 heterodimers. While it is tempting to speculate that such heterodimers may contribute some novel function, their existence at high levels would undermine the ability of cells to satisfy ongoing demands for Qk activity for splicing (or translation) due to normal fluctuation of Qk5 levels in the nucleus (or Qk6 levels in the cytoplasm). The independent control of Qk in each compartment would be lost, because isoform identity is blurred in heterodimers. The need to limit heterodimer levels may be one reason that typically either Qk5 or Qk6 but not both are highly expressed in the same cell, a condition that disrupts the isoform division of labor (Figs 2-5 and 7).

Auto- and cross isoform regulation balances quantitative output from the Qk gene

To identify processes that require specific isoforms in the presence of others, we sought to deplete cells of each single isoform of Qk protein in turn, to confirm the distinct function(s) of each. This effort was made more challenging by the strong dependence of Qk6 expression on expression of Qk5 (Fig 3). In analyzing the effect of depleting each Qk isoform on the expression of RNA and protein for itself and the other Qk isoforms, we found that Qk5 is required for nuclear accumulation of both its own transcripts and those encoding Qk6/7 (Fig 4). We also provide evidence that Qk6 represses translation of Qk5 mRNA but activates translation of its own mRNA (Fig 5). These results allowed us to build a model of Qk autogenous and cross-isoform regulation for C2C12 cells (Fig 7A), that also applies in cell types with a lower Qk5:Qk6 ratio than C2C12 myoblasts

(Fig 6). This control network is more similar to a rheostat than a bistable switch where either Qk5 or Qk6 expression dominates, because it supports stable intermediate isoform mixtures from the *Qk* gene in different cell types (Fig 7A). The structure of this network is such that the same compartmentalization that constrains the functional role of each isoform is also used to create the auto- and cross-regulatory controls. Qk5 acts on its own RNA and that of Qk6/7 through nuclear processes, whereas Qk6 acts on both its own mRNA and that of Qk5 through translation and decay in the cytoplasm. This network controls both the total amount of Qk protein by combining a strong dependence of Qk6 expression on Qk5 with negative feedback of Qk5 by both Qk5 (at the RNA level) and Qk6 (at the translational level). Autoregulation by RBPs is common and can be imposed at different RNA processing steps including splicing (Wollerton et al. 2004; Lareau et al. 2007; Ni et al. 2007), polyadenylation (Dai et al. 2012), mRNA stability/decay (Ayala et al. 2011), and translation (de Melo Neto et al. 1995; Wu and Bag 1998). Although cross-paralog regulation exists between RBP family members encoded by separate genes (Boutz PL 2007; Spellman et al. 2007; Wang et al. 2012)), the Qk regulatory network highlights the role of compartmentalization in both functional specification and role in the regulatory network of RBP isoforms (Fig 7). Other RBP families may use similar mechanisms for autogenous and cross-isoform control but for those encoded by multiple genes, additional feedback on transcription are possible and may be necessary.

Since the quantitative output from the Qk network appears to be set at different Qk5:Qk6:Qk7 ratios in different cell types (Fig 6A), it must also be sensitive to regulation by other factors. For example, the RBP RBFOX2 reduces Qk7 expression by repressing alternative splicing in human embryonic stem cells (Yeo et al. 2009). Since

RbFox2 is an abundant splicing regulator in C2C12 cells (Bland et al. 2010; Singh et al. 2014), this may explain why Qk7 is nearly undetectable (Figs S1A and 6A). This seems not to hold in mouse cerebellum, where both Qk7 (Fig 6A) and RbFox2 (Gehman et al. 2012) are abundant, therefore yet other cell-type specific factors are likely present. In another example, miR-214-3p targets regions common to both the Qk6 and Qk7 3'UTR (van Mil et al. 2012) that are not present in the Qk5 3'UTR, consequently downregulating Qk6 and Qk7 (Irie et al. 2016). There likely are additional means by which Qk isoform ratios can be regulated, but the Qk auto- and cross-regulatory isoform network uncovered here may represent the foundational structure on which that regulation is imposed.

Qk isoform ratio regulation, development, and cancer

Qk is a key regulator of development (Ebersole et al. 1996; Li et al. 2003; Justice and Hirschi 2010) and cancer (Novikov et al. 2011; Chen et al. 2012; Zong et al. 2014). Our model predicts that Qk5 expression precedes expression of other Qk isoforms temporally as transcription is upregulated at the *Qk* gene (Fig 7B), either during cancer progression or in a developmental context. This expectation appears to hold for embryogenesis in *Xenopus* (Zorn et al. 1997), zebrafish (Radomska et al. 2016), and mouse (Ebersole et al. 1996; Hardy et al. 1996). Additionally, early stem/progenitor cells in *Drosophila* (Nabel-Rosen et al. 1999) and mice (Hardy 1998), express predominantly Qk5 (or its ortholog HowL in *Drosophila*). In mice, *qk* knockout is embryonic lethal (Li et al. 2003) and the qk^{l1} mutant mouse, which appears to lack Qk5 expression due to disruption of Qk5-specific splicing by a point mutation (Cox et al. 1999), is recessive lethal (Shedlovsky et al. 1988). In this mutant, both Qk6 and Qk7 mRNAs are

significantly reduced in visceral endoderm dissected from non-viable embryos (Cox et al. 1999; Bohnsack et al. 2006), suggesting that Qk5 is required for efficient Qk6 and Qk7 expression in this tissue also. These observations provide additional evidence in support of our model of *Qk* autoregulation, and suggest its importance in an evolutionarily conserved developmental context.

The extensively studied qk^{v} mouse model of dysmyelination (Sidman et al. 1964) expresses reduced mRNA levels of all Qk isoforms in glia (Lu et al. 2003) and vascular smooth muscle (van der Veer et al. 2013), due to a deletion that includes a portion of the *Qk* promoter (Ebersole et al. 1996). Based on the models we present here (Fig 7), lower Qk5 protein levels in qk^{v} oligodendrocyte precursor cells may be insufficient for robust Qk6 and Qk7 up-regulation that normally occurs around the peak of myelination (Ebersole et al. 1996). Since deletion of *qk* in oligodendrocytes is lethal (Darbelli et al. 2016), the reduction in Qk6 and Qk7 in qk^{v} oligodendrocytes could be due to selective pressure imposed on Qk5 substrates to maintain viability of the organism. Therefore, the imbalance of Qk isoforms in qk^{v} oligodendrocytes results in developmental defects and the tremor phenotype without sacrificing viability of the organism.

Finally, disruption of tissue-specific Qk isoform expression patterns is also observed in non-small-cell lung cancer (NSCLC) (Sebestyen et al. 2015; de Miguel et al. 2016) and glioblastoma (Xi et al. 2017) patient samples. Although overall Qk is reduced, an isoform ratio switch occurs whereby healthy lung cells expressing mostly Qk6 transition to a state in NSCLC samples where cells express predominantly Qk5 (Sebestyen et al. 2015; de Miguel et al. 2016). This isoform switch likely shifts *QKI* function away from cytoplasmic regulation such as translation and decay (Saccomanno L

1999; Zhao et al. 2010; Figs 5 and 6), toward nuclear processes such as splicing (Figs 2B, 3B, 3C, 4C, and 4D) and primary transcript stability (Fig 4B). Understanding the relationship of *QKI* gene function in the context of cancer and other diseases requires evaluation of both the specific functions of Qk protein isoforms on their own RNAs as well as on the other pre-mRNAs and mRNAs from the many other genes that *QKI* regulates.

Materials and Methods

Cell Culture, Lysis, and Transfections

C2C12 cells were routinely cultured in Dulbecco's modified Eagle medium (DMEM) with high glucose (Life Technologies) supplemented with 10% heat inactivated fetal bovine serum (Life Technologies) at 37°C with 5% CO_2. For differentiation experiments, C2C12 cells were allowed to reach ~90% confluency, then the media was changed to DMEM supplemented with 5% horse serum (Life Technologies) and the cells were harvested 72h post media change. C6 glioma cells were cultured in F-12K media (ATCC) supplemented with fetal bovine serum at 2.5% and horse serum at 15% as described (Benda et al. 1968) at 37°C with 5% CO_2. CG4 oligodendrocyte precursor cells were grown in DMEM with high glucose supplemented with N1 (5 µg/ml transferrin, 100 µM putrescine, 20 nM progesterone, and 20 nM selenium), biotin (10 ng/ml), insulin (5 µg/ml), and 30% B104 cell conditioned media as described (Louis et al. 1992) at 37°C with 5% CO_2; all supplements purchased from Sigma-Aldrich. Protein lysates were prepared by directly lysing cells in a buffer consisting of 100 mM Tris-HCl pH 7.4, 0.5% NP-40, 0.5% Triton X-100, 0.1% SDS, 100 mM NaCl, and 2.5 mM $MgCl_2$. Cell lysis and

analysis of luciferase protein expression for 3'UTR reporter assays were performed using the Dual Glo Luciferase Assay system (Promega) according to the manufacturer's instructions (luciferase reporter RNA could not be accurately measured due to persistent contaminating plasmid DNA resistant to DNase treatment). RNA extraction was performed using TriZOL reagent (Life Technologies) according to the manufacturer's suggestions and genomic DNA was degraded using Turbo DNase (Life Technologies) according to the manufacturer's specifications. Transfections were performed using the Lipofectamine2000 reagent (Life Technologies) according to the manufacturer's specifications.

Additional methods and oligonucleotide sequences found in Supplemental Information.

Acknowledgements

We thank Sean Ryder, Doug Black, Jeremy Sanford, Rhonda Perriman, David Feldheim, and Susan Strome for reagents, discussion, and advice. This work was supported by National Institutes of Health (NIH) grant R01-GM040478 to M.A., NIH pre-doctoral T32 GM008646 to WSF, and California Institute of Regenerative Medicine (CIRM) pre-doctoral fellowship award TG2-01157 to WSF.

References

Aberg K, Saetre P, Jareborg N, Jazin E. 2006. Human QKI, a potential regulator of mRNA expression of human oligodendrocyte-related genes involved in schizophrenia. *Proceedings of the National Academy of Sciences of the United States of America* **103**: 7482-7487.

Ayala YM, De Conti L, Avendano-Vazquez SE, Dhir A, Romano M, D'Ambrogio A, Tollervey J, Ule J, Baralle M, Buratti E et al. 2011. TDP-43 regulates its mRNA levels through a negative feedback loop. *The EMBO journal* **30**: 277-288.

Benda P, Lightbody J, Sato G, Levine L, Sweet W. 1968. Differentiated rat glial cell strain in tissue culture. *Science (New York, NY)* **161**: 370-371.

Benda P, Someda K, Messer J, Sweet WH. 1971. Morphological and immunochemical studies of rat glial tumors and clonal strains propagated in culture. *Journal of neurosurgery* **34**: 310-323.

Beuck C, Qu S, Fagg WS, Ares M, Jr., Williamson JR. 2012. Structural analysis of the Quaking homodimerization interface. *J Mol Biol*.

Bland CS, Wang ET, Vu A, David MP, Castle JC, Johnson JM, Burge CB, Cooper TA. 2010. Global regulation of alternative splicing during myogenic differentiation. *Nucleic acids research* **38**: 7651-7664.

Bohnsack BL, Lai L, Northrop JL, Justice MJ, Hirschi KK. 2006. Visceral endoderm function is regulated by quaking and required for vascular development. *Genesis (New York, NY : 2000)* **44**: 93-104.

Boutz PL SP, Li Q, Lin CH, Chawla G, Ostrow K, Shiue L, Ares M Jr, Black DL. 2007. A post-transcriptional regulatory switch in polypyrimidine tract-binding proteins reprograms alternative splicing in developing neurons. *Genes and Development* **21**: 1636-1652.

Caceres JF, Screaton GR, Krainer AR. 1998. A specific subset of SR proteins shuttles continuously between the nucleus and the cytoplasm. *Genes & development* **12**: 55-66.

Cazalla D, Zhu J, Manche L, Huber E, Krainer AR, Caceres JF. 2002. Nuclear export and retention signals in the RS domain of SR proteins. *Molecular and cellular biology* **22**: 6871-6882.

Charizanis K, Lee KY, Batra R, Goodwin M, Zhang C, Yuan Y, Shiue L, Cline M, Scotti MM, Xia G et al. 2012. Muscleblind-like 2-Mediated Alternative Splicing in the Developing Brain and Dysregulation in Myotonic Dystrophy. *Neuron* **75**: 437-450.

Cheever A, Ceman S. 2009. Phosphorylation of FMRP inhibits association with Dicer. *RNA (New York, NY)* **15**: 362-366.

Chen AJ, Paik JH, Zhang H, Shukla SA, Mortensen R, Hu J, Ying H, Hu B, Hurt J, Farny N et al. 2012. STAR RNA-binding protein Quaking suppresses cancer via stabilization of specific miRNA. *Genes & development* **26**: 1459-1472.

Cook AG, Conti E. 2010. Nuclear export complexes in the frame. *Current opinion in structural biology* **20**: 247-252.

Cox RD, Hugill A, Shedlovsky A, Noveroske JK, Best S, Justice MJ, Lehrach H, Dove WF. 1999. Contrasting effects of ENU induced embryonic lethal mutations of the quaking gene. *Genomics* **57**: 333-341.

Dai W, Zhang G, Makeyev EV. 2012. RNA-binding protein HuR autoregulates its expression by promoting alternative polyadenylation site usage. *Nucleic acids research* **40**: 787-800.

Damianov A, Black DL. 2010. Autoregulation of Fox protein expression to produce dominant negative splicing factors. *RNA (New York, NY)* **16**: 405-416.

Darbelli L, Vogel G, Almazan G, Richard S. 2016. Quaking Regulates Neurofascin 155 Expression for Myelin and Axoglial Junction Maintenance. *The Journal of neuroscience : the official journal of the Society for Neuroscience* **36**: 4106-4120.

de Bruin RG, Shiue L, Prins J, de Boer HC, Singh A, Fagg WS, van Gils JM, Duijs JM, Katzman S, Kraaijeveld AO et al. 2016a. Quaking promotes monocyte differentiation into pro-atherogenic macrophages by controlling pre-mRNA splicing and gene expression. *Nature communications* **7**: 10846.

de Bruin RG, van der Veer EP, Prins J, Lee DH, Dane MJ, Zhang H, Roeten MK, Bijkerk R, de Boer HC, Rabelink TJ et al. 2016b. The RNA-binding protein quaking maintains endothelial barrier function and affects VE-cadherin and beta-catenin protein expression. *Scientific reports* **6**: 21643.

de Melo Neto OP, Standart N, Martins de Sa C. 1995. Autoregulation of poly(A)-binding protein synthesis in vitro. *Nucleic acids research* **23**: 2198-2205.

de Miguel FJ, Pajares MJ, Martinez-Terroba E, Ajona D, Morales X, Sharma RD, Pardo FJ, Rouzaut A, Rubio A, Montuenga LM et al. 2016. A large-scale analysis of alternative splicing reveals a key role of QKI in lung cancer. *Molecular oncology* **10**: 1437-1449.

Dominski Z, Kole R. 1991. Selection of splice sites in pre-mRNAs with short internal exons. *Mol Cell Biol* **11**: 6075-6083.

Ebersole TA, Chen Q, Justice MJ, Artzt K. 1996. The quaking gene product necessary in embryogenesis and myelination combines features of RNA binding and signal transduction proteins. *Nature Genetics* **12**: 260-265.

Fu XD, Ares M, Jr. 2014. Context-dependent control of alternative splicing by RNA-binding proteins. *Nature reviews Genetics* **15**: 689-701.

Galarneau A, Richard S. 2005. Target RNA motif and target mRNAs of the Quaking STAR protein. *Nature structural & molecular biology* **12**: 691-698.

Gehman LT, Meera P, Stoilov P, Shiue L, O'Brien JE, Meisler MH, Ares M, Jr., Otis TS, Black DL. 2012. The splicing regulator Rbfox2 is required for both cerebellar development and mature motor function. *Genes & development* **26**: 445-460.

Gehman LT, Stoilov P, Maguire J, Damianov A, Lin CH, Shiue L, Ares M, Jr., Mody I, Black DL. 2011. The splicing regulator Rbfox1 (A2BP1) controls neuronal excitation in the mammalian brain. *Nat Genet* **43**: 706-711.

Hafner M, Landthaler M, Burger L, Khorshid M, Hausser J, Berninger P, Rothballer A, Ascano M, Jr., Jungkamp AC, Munschauer M et al. 2010. Transcriptome-wide identification of RNA-binding protein and microRNA target sites by PAR-CLIP. *Cell* **141**: 129-141.

Hall MP, Nagel RJ, Fagg WS, Shiue L, Cline MS, Perriman RJ, Donohue JP, Ares M, Jr. 2013. Quaking and PTB control overlapping splicing regulatory networks during muscle cell differentiation. *RNA (New York, NY)* **19**: 627-638.

Hamada N, Ito H, Iwamoto I, Mizuno M, Morishita R, Inaguma Y, Kawamoto S, Tabata H, Nagata K. 2013. Biochemical and morphological characterization of A2BP1 in neuronal tissue. *Journal of neuroscience research* **91**: 1303-1311.

Hardy RJ. 1998. QKI expression is regulated during neuron-glial cell fate decisions. *Journal of neuroscience research* **54**: 46-57.

Hardy RJ, Loushin CL, Friedrich Jr VL, Chen Q, Ebersole TA, Lazzarini RA, Artzt K. 1996. Neural Cell Type-Specific Expression of QKI Proteins Is Altered in quakingviable Mutant Mice. *J Neurosci* **16**: 7941-7949.

Irie K, Tsujimura K, Nakashima H, Nakashima K. 2016. MicroRNA-214 Promotes Dendritic Development by Targeting the Schizophrenia-associated Gene Quaking (Qki). *The Journal of biological chemistry* **291**: 13891-13904.

Jin P, Zarnescu DC, Ceman S, Nakamoto M, Mowrey J, Jongens TA, Nelson DL, Moses K, Warren ST. 2004. Biochemical and genetic interaction between the fragile X mental retardation protein and the microRNA pathway. *Nature neuroscience* **7**: 113-117.

Justice MJ, Hirschi KK. 2010. The role of quaking in mammalian embryonic development. *Advances in experimental medicine and biology* **693**: 82-92.

Kawai T, Fan J, Mazan-Mamczarz K, Gorospe M. 2004. Global mRNA stabilization preferentially linked to translational repression during the endoplasmic reticulum stress response. *Molecular and cellular biology* **24**: 6773-6787.

Keene JD. 2007. RNA regulons: coordination of post-transcriptional events. *Nature reviews Genetics* **8**: 533-543.

Koizumi J, Okamoto Y, Onogi H, Mayeda A, Krainer AR, Hagiwara M. 1999. The subcellular localization of SF2/ASF is regulated by direct interaction with SR protein kinases (SRPKs). *The Journal of biological chemistry* **274**: 11125-11131.

Kondo T, Furuta T, Mitsunaga K, Ebersole TA, Shichiri M, Wu J, Artzt K, Yamamura K, Abe K. 1999. Genomic organization and expression analysis of the mouse qkI locus. *Mammalian genome : official journal of the International Mammalian Genome Society* **10**: 662-669.

Lareau LF, Inada M, Green RE, Wengrod JC, Brenner SE. 2007. Unproductive splicing of SR genes associated with highly conserved and ultraconserved DNA elements. *Nature* **446**: 926-929.

Larocque D, Galarneau A, Liu H-N, Scott M, Almazan G, Richard S. 2005. Protection of p27Kip1 mRNA by quaking RNA binding proteins promotes oligodendrocyte differentiation. *Nat Neurosci* **8**: 27-33.

Larocque D, Pilotte J, Chen T, Cloutier F, Massie B, Pedraza L, Couture R, Lasko P, Almazan G, Richard S. 2002. Nuclear Retention of MBP mRNAs in the Quaking Viable Mice. *Neuron* **36**: 815-829.

Lee JA, Damianov A, Lin CH, Fontes M, Parikshak NN, Anderson ES, Geschwind DH, Black DL, Martin KC. 2016. Cytoplasmic Rbfox1 Regulates the Expression of Synaptic and Autism-Related Genes. *Neuron* **89**: 113-128.

Lee JA, Tang ZZ, Black DL. 2009. An inducible change in Fox-1/A2BP1 splicing modulates the alternative splicing of downstream neuronal target exons. *Genes & development* **23**: 2284-2293.

Li Z, Takakura N, Oike Y, Imanaka T, Araki K, Suda T, Kaname T, Kondo T, Abe K, Yamamura K. 2003. Defective smooth muscle development in qkI-deficient mice. *Development, growth & differentiation* **45**: 449-462.

Li Z, Zhang Y, Li D, Feng Y. 2000. Destabilization and Mislocalization of Myelin Basic Protein mRNAs in quaking Dysmyelination Lacking the QKI RNA-Binding Proteins. *J Neurosci* **20**: 4944-4953.

Louis JC, Magal E, Muir D, Manthorpe M, Varon S. 1992. CG-4, a new bipotential glial cell line from rat brain, is capable of differentiating in vitro into either mature oligodendrocytes or type-2 astrocytes. *Journal of neuroscience research* **31**: 193-204.

Lu Z, Zhang Y, Ku L, Wang H, Ahmadian A, Feng Y. 2003. The quakingviable mutation affects qkI mRNA expression specifically in myelin-producing cells of the nervous system. *Nucleic acids research* **31**: 4616-4624.

Makeyev EV, Zhang J, Carrasco MA, Maniatis T. 2007. The MicroRNA miR-124 Promotes Neuronal Differentiation by Triggering Brain-Specific Alternative Pre-mRNA Splicing. *Molecular cell* **27**: 435-448.

Nabel-Rosen H, Dorevitch N, Reuveny A, Volk T. 1999. The balance between two isoforms of the Drosophila RNA-binding protein how controls tendon cell differentiation. *Molecular cell* **4**: 573-584.

Nabel-Rosen H, Volohonsky G, Reuveny A, Zaidel-Bar R, Volk T. 2002. Two Isoforms of the Drosophila RNA Binding Protein, How, Act in Opposing Directions to Regulate Tendon Cell Differentiation. *Developmental Cell* **2**: 183-193.

Nakielny S, Dreyfuss G. 1999. Transport of proteins and RNAs in and out of the nucleus. *Cell* **99**: 677-690.

Ni JZ, Grate L, Donohue JP, Preston C, Nobida N, O,ÄôBrien G, Shiue L, Clark TA, Blume JE, Ares M. 2007. Ultraconserved elements are associated with homeostatic control of splicing regulators by alternative splicing and nonsense-mediated decay. *Genes & development* **21**: 708-718.

Novikov L, Park JW, Chen H, Klerman H, Jalloh AS, Gamble MJ. 2011. QKI-mediated alternative splicing of the histone variant MacroH2A1 regulates cancer cell proliferation. *Molecular and cellular biology* **31**: 4244-4255.

Paz I, Kosti I, Ares M, Jr., Cline M, Mandel-Gutfreund Y. 2014. RBPmap: a web server for mapping binding sites of RNA-binding proteins. *Nucleic acids research* **42**: W361-367.

Pilotte J, Larocque D, Richard S. 2001. Nuclear translocation controlled by alternatively spliced isoforms inactivates the QUAKING apoptotic inducer. *Genes & development* **15**: 845-858.

Radomska KJ, Sager J, Farnsworth B, Tellgren-Roth A, Tuveri G, Peuckert C, Kettunen P, Jazin E, Emilsson LS. 2016. Characterization and Expression of the Zebrafish qki Paralogs. *PloS one* **11**: e0146155.

Roscigno RF, Garcia-Blanco MA. 1995. SR proteins escort the U4/U6.U5 tri-snRNP to the spliceosome. *RNA (New York, NY)* **1**: 692-706.

Ryder SP, Williamson JR. 2004. Specificity of the STAR/GSG domain protein Qk1: Implications for the regulation of myelination. *RNA (New York, NY)* **10**: 1449-1458.

Saccomanno L LC, Jan E, Punkay E, Artzt K, and Goodwin EB. 1999. The STAR protein QKI-6 is a translational repressor. *Proceedings of the National Academy of Sciences of the United States of America* **96**: 12605-12610.

Sanford JR, Gray NK, Beckmann K, Caceres JF. 2004. A novel role for shuttling SR proteins in mRNA translation. *Genes & development* **18**: 755-768.

Sebestyen E, Zawisza M, Eyras E. 2015. Detection of recurrent alternative splicing switches in tumor samples reveals novel signatures of cancer. *Nucleic acids research* **43**: 1345-1356.

Sen GL, Blau HM. 2005. Argonaute 2/RISC resides in sites of mammalian mRNA decay known as cytoplasmic bodies. *Nature cell biology* **7**: 633-636.

Sharma S, Maris C, Allain FH, Black DL. 2011. U1 snRNA directly interacts with polypyrimidine tract-binding protein during splicing repression. *Molecular cell* **41**: 579-588.

Shedlovsky A, King TR, Dove WF. 1988. Saturation germ line mutagenesis of the murine t region including a lethal allele at the quaking locus. *Proceedings of the National Academy of Sciences of the United States of America* **85**: 180-184.

Sidman R, Dickie M, Appel S. 1964. Mutant mice (quaking and jimpy) with deficient myelination in the central nervous system. *Science (New York, NY)* **144**: 309-311.

Singh RK, Xia Z, Bland CS, Kalsotra A, Scavuzzo MA, Curk T, Ule J, Li W, Cooper TA. 2014. Rbfox2-coordinated alternative splicing of Mef2d and Rock2 controls myoblast fusion during myogenesis. *Molecular cell* **55**: 592-603.

Spellman R, Llorian M, Smith CWJ. 2007. Crossregulation and Functional Redundancy between the Splicing Regulator PTB and Its Paralogs nPTB and ROD1. *Molecular cell* **27**: 420-434.

Sun S, Zhang Z, Sinha R, Karni R, Krainer AR. 2010. SF2/ASF autoregulation involves multiple layers of post-transcriptional and translational control. *Nature structural & molecular biology* **17**: 306-312.

Teplova M, Hafner M, Teplov D, Essig K, Tuschl T, Patel DJ. 2013. Structure-function studies of STAR family Quaking proteins bound to their in vivo RNA target sites. *Genes & development* **27**: 928-940.

Underwood JG, Boutz PL, Dougherty JD, Stoilov P, Black DL. 2005. Homologues of the Caenorhabditis elegans Fox-1 protein are neuronal splicing regulators in mammals. *Molecular and cellular biology* **25**: 10005-10016.

van der Veer EP, de Bruin RG, Kraaijeveld AO, de Vries MR, Bot I, Pera T, Segers FM, Trompet S, van Gils JM, Roeten MK et al. 2013. Quaking, an RNA-binding protein, is a critical regulator of vascular smooth muscle cell phenotype. *Circulation research* **113**: 1065-1075.

van Mil A, Grundmann S, Goumans MJ, Lei Z, Oerlemans MI, Jaksani S, Doevendans PA, Sluijter JP. 2012. MicroRNA-214 inhibits angiogenesis by targeting Quaking and reducing angiogenic growth factor release. *Cardiovasc Res* **93**: 655-665.

Van Nostrand EL, Pratt GA, Shishkin AA, Gelboin-Burkhart C, Fang MY, Sundararaman B, Blue SM, Nguyen TB, Surka C, Elkins K et al. 2016. Robust transcriptome-wide discovery of RNA-binding protein binding sites with enhanced CLIP (eCLIP). *Nature methods* **13**: 508-514.

Vasudevan S, Steitz JA. 2007. AU-rich-element-mediated upregulation of translation by FXR1 and Argonaute 2. *Cell* **128**: 1105-1118.

Wang ET, Cody NA, Jog S, Biancolella M, Wang TT, Treacy DJ, Luo S, Schroth GP, Housman DE, Reddy S et al. 2012. Transcriptome-wide Regulation of Pre-mRNA Splicing and mRNA Localization by Muscleblind Proteins. *Cell* **150**: 710-724.

Wang Y, Vogel G, Yu Z, Richard S. 2013. The QKI-5 and QKI-6 RNA binding proteins regulate the expression of microRNA 7 in glial cells. *Molecular and cellular biology* **33**: 1233-1243.

Wollerton MC, Gooding C, Wagner EJ, Garcia-Blanco MA, Smith CW. 2004. Autoregulation of polypyrimidine tract binding protein by alternative splicing leading to nonsense-mediated decay. *Molecular cell* **13**: 91-100.

Wu J, Bag J. 1998. Negative control of the poly(A)-binding protein mRNA translation is mediated by the adenine-rich region of its 5'-untranslated region. *The Journal of biological chemistry* **273**: 34535-34542.

Wu J, Zhou L, Tonissen K, Tee R, Artzt K. 1999. The Quaking I-5 Protein (QKI-5) Has a Novel Nuclear Localization Signal and Shuttles between the Nucleus and the Cytoplasm. *J Biol Chem* **274**: 29202-29210.

Wu JI, Reed RB, Grabowski PJ, Artzt K. 2002. Function of quaking in myelination: Regulation of alternative splicing. *Proceedings of the National Academy of Sciences of the United States of America* **99**: 4233-4238.

Xi Z, Wang P, Xue Y, Shang C, Liu X, Ma J, Li Z, Li Z, Bao M, Liu Y. 2017. Overexpression of miR-29a reduces the oncogenic properties of glioblastoma stem cells by downregulating Quaking gene isoform 6. *Oncotarget*.

Yaffe D, Saxel O. 1977. Serial passaging and differentiation of myogenic cells isolated from dystrophic mouse muscle. *Nature* **270**: 725-727.

Yeo GW, Coufal NG, Liang TY, Peng GE, Fu XD, Gage FH. 2009. An RNA code for the FOX2 splicing regulator revealed by mapping RNA-protein interactions in stem cells. *Nature structural & molecular biology* **16**: 130-137.

Zearfoss NR, Clingman CC, Farley BM, McCoig LM, Ryder SP. 2011. Quaking regulates Hnrnpa1 expression through its 3' UTR in oligodendrocyte precursor cells. *PLoS genetics* **7**: e1001269.

Zhao L, Mandler MD, Yi H, Feng Y. 2010. Quaking I controls a unique cytoplasmic pathway that regulates alternative splicing of myelin-associated glycoprotein. *Proceedings of the National Academy of Sciences of the United States of America* **107**: 19061-19066.

Zong FY, Fu X, Wei WJ, Luo YG, Heiner M, Cao LJ, Fang Z, Fang R, Lu D, Ji H et al. 2014. The RNA-binding protein QKI suppresses cancer-associated aberrant splicing. *PLoS genetics* **10**: e1004289.

Zorn AM, Grow M, Patterson KD, Ebersole TA, Chen Q, Artzt K, Krieg PA. 1997. Remarkable sequence conservation of transcripts encoding amphibian and mammalian homologues of quaking, a KH domain RNA-binding protein. *Gene* **188**: 199-206.

Figure 1: Qk5 and Qk6 are the predominant isoforms and can activate splicing in C2C12 muscle cells A. Cartoon model depicting endogenous Qk protein isoforms (top) with number of unique amino acids shown at C-terminus (right), and Myc-epitope tagged constructs (bottom) used in subsequent experiments; all Qk proteins share the same 311 amino acids including Quaking homology 1 (Qua1) and 2 (Qua2), and hnRNP-K homology (KH) domains. B. Western blot of whole cell extracts prepared from undifferentiated C2C12 myoblasts (UD) or C2C12 cells differentiated for 72h (72h) simultaneously probed with infrared-conjugated secondary antibodies to Qk5 (top), Qk6 (middle), or Qk7 (bottom) in the red channel (notation to the right indicates migration of specific isoform) or PanQk (green channel), which recognizes all Qk isoforms. C. Indirect immunofluorescence showing PanQk antibody staining in green and DAPI staining in blue in undifferentiated C2C12 myoblasts (left, arrows show nuclei from individual cells) or differentiated C2C12 myotube (right, arrowheads show three nuclei in single myotube); scale bar represents 4.8 μm. D. Indirect immunofluorescent analysis of endogenous Qk5 (left, red), Qk6 (middle, red), or Qk7 (right, red), and DAPI (blue) to stain nuclei; bottom panels show all 3 channels overlaid; scale bar represents 10 μm. E. Indirect immunofluorescence of C2C12 myoblasts transfected with either Myc-Qk5 (left) or Myc-Qk6 (right) stained using Anti-Myc epitope antibody in red (top), DAPI in blue (middle), and both channels overlaid (bottom); scale bar represents 8 μm. F. RT-PCR products from pDup51-Capzb exon 9 splicing reporter analyzed on BioAnalyzer from RNA extracted from C2C12 myoblasts either mock transfected, or transfected with Myc-Qk5 or Myc-Qk6 plasmid; mean values of percent included are shown below (+/- standard deviation) from three independent biological replicates.

Figure S1 (supplemental to Figure 1): A. Representative western blot of whole cell extracts prepared from C2C12 myoblasts transfected as described in Fig 1E and 1F probed simultaneously with PanQk antibody (top; notation to the right indicates observed protein migration pattern) and Gapdh (bottom). B. Representative western blot of whole cell extracts prepared from C2C12 myoblasts transfected with control siRNA (siNT), or siRNA targeting all Qk isoforms (siQk), siQk plus Myc-Qk5, and siQk plus Myc-Qk6 Myc epitope antibody (top), Qk5 antibody (second from top), Qk6 antibody (second from bottom), and Gapdh antibody (bottom).

Figure 2: Nuclear localization is sufficient for Qk splicing function. A. Cartoon model of Myc epitope-tagged Qk5 and Qk6 with number of unique amino acids shown at C-terminus. B. RT-PCR products from pDup51-Capzb exon 9 splicing reporter analyzed on BioAnalyzer from RNA extracted from C2C12 myoblasts transfected with either control siRNA (siNT) or siRNA targeting all Qk isoforms (siQk), or co-transfected with both siQk and Myc-Qk5 or siQk and Myc-Qk6 (top); mean value of percent included is shown below from three independent biological replicates with standard deviation shown below. C. Indirect immunofluorescence using Anti-Myc epitope antibody in red (top), DAPI in blue (middle), and channels overlaid (bottom) of C2C12 myoblasts transfected with siQk + Myc-Qk5 (left) or siQk + Myc-Qk6 (right); scale bar represents 8 μm. D. Cartoon model of Qk mutant proteins tested for splicing function and localization: HA-QkBody consists of an N-terminal HA epitope tag and the 311 amino acids common to all Qk proteins (top) and HA-NLS-QkBody consists of an N-terminal HA tag and NLS from SV40 preceding the common 311 amino acids to all Qk isoforms (bottom). E. RT-PCR products from Capzb exon 9 splicing reporter analyzed on BioAnalyzer from RNA extracted from C2C12 myoblasts transfected with siNT, siNT and HA-QkBody, siNT and HA-NLS-QkBody, siQk, siQk and HA-QkBody, or siQk and HA-NLS-QkBody (left to right); mean percent included from three independent biological replicates with standard deviation shown below. F. Indirect immunofluorescence using HA antibody (top, red), DAPI staining (blue, middle), and overlaid images at bottom of representative C2C12 myoblasts from siNT + HA-QkBody, siNT + HA-NLS-QkBody, siQk + HA-QkBody, and siQk + HA-NLS-QkBody transfections (left to right); scale bar represents 8 μm.

Figure S2 (supplemental to Figure 2): A. Representative western blot of protein lysates from C2C12 myoblast transfections described in Fig 2E and 2F: top shows blot probed with PanQk antibody (observed migration pattern of endogenous and mutant proteins shown at right), middle probed with HA epitope antibody, and bottom probed with Gapdh antibody.

Figure 3: Qk5 is required for splicing and Qk6 RNA expression. A. UCSC Genome Browser screen shot showing RefSeq Genes (top) with Qk5, Qk6, and Qk7 isoforms noted on right and Mammalian Conservation (bottom) tracks; arrows show approximate region targeted with Qk6&7 siRNA and three different siRNAs targeting Qk5 (Qk5 siRNA1, Qk5 siRNA2, and Qk5 siRNA3). B. Representative agarose gel analyzing RT-PCR products from endogenous Rai14 exon 11 from RNA extracted from C2C12 myoblasts transfected with siNT, siQk5-1, or siQk6&7. C. RT-PCR products from Dup-Capzb exon 9 splicing reporter analyzed on BioAnalyzer from RNA extracted from C2C12 myoblasts transfected with siNT, siQk5-1, and siQk6/7; mean percent included from 3 biological replicates +/- standard deviation is shown below (** $p < 0.01$; * $p < 0.05$ by student's t-test). D. Western blot of protein extracted from C2C12 myoblasts transfected with siNT, siQk, siQk5-1, and siQk6/7 probed simultaneously with anti-PanQk and anti-Gapdh (notation at right shows migration pattern of Qk protein isoforms). E. RT-qPCR analysis of RNA extracted from C2C12 myoblast cultures transfected with siNT, siQk5-1, siQk5-2, or siQk5-3 for Qk5 (left) or Qk6/7 (right) RNA normalized to Mapk3 RNA and displayed as fold change relative to siNT; error bars show standard deviation from the mean using three independent biological replicates.

Figure S3 (supplemental to Figure 3): A. Western blots simultaneously probed with Qk6 and Gapdh (top) or Qk7 and Gapdh (bottom) antibodies from whole cell protein lysate from C2C12 myoblasts transfected with siNT, siQk5-1, and siQk6/7; mean percentage of protein abundance relative to siNT is shown below from three independent biological replicates, +/- standard deviation from the mean. B. Representative western blot simultaneously probed with Qk5 and Gapdh (top) or Qk6 and Gapdh (bottom) antibodies from whole cell protein extracted from C2C12 myoblasts transfected with siNT, siQk5-1, siQk5-2, and siQk5-3 (as in Fig 3E). C. UCSC Genome Browser screen shot showing genomic region including Qk5 pre-mRNA (top), a portion of the Qk7 3'UTR (middle), and Qk6 3'UTR (bottom), with RBP Map predicted Qk binding sites, peaks from PanQKI eCLIP experiments performed in HepG2 and K562 cells, a peak from tagged QKI PAR-CLIP experiment performed in HEK293T cells, and mammalian conservation track. D. Schematic of Qk6 3'UTR dual luciferase assay (left) and representative western blot (right) from three independent replicate experiments using whole cell extracts from C2C12 myoblasts transfected with renilla luciferase-Qk6-3'UTR reporter and firefly luciferase with either siNT, siQk, or siQk5-1 probed with PanQk and Gapdh antibodies. E. Whole cell lysate from C2C12 myoblasts transfected as described in S3D analyzed for luciferase abundance: renilla luciferase normalized to firefly luciferase and expressed as fold change relative to siNT control; error bars represent the standard deviation from the mean of three independent biological replicates.

Figure 4: Qk5 is required for nuclear accumulation of Qk RNAs by promoting its own 3' splice site usage. A. Representative western blot of protein lysates from whole cell extract (WCE, left) or nuclear fraction (nuclear, right) C2C12 myoblasts transfected with siNT, siQk5-1, and siQk6/7 probed with antibodies against PanQk, histone H3, and Gapdh. B. RT-qPCR performed on nuclear RNA extracted from C2C12 myoblasts transfected with siNT and siQk5-1 measuring Qk5 RNA (left) and Qk6/7 RNA (right; note primer set also amplifies a region of Qk5 intron, see methods section) normalized to 7SK RNA and reported as fold change relative to siNT (error bars represent standard deviation from the mean of 3 biological replicates). C. RT-qPCR performed on nuclear RNA extracted from C2C12 myoblasts transfected in biological triplicate with siNT, siQk5-1, and siQk6/7; left side shows unspliced Qk5 RNA normalized to total Qk5 RNA and right side shows read-through Qk5 RNA relative to total Qk5 RNA, both are reported as fold change relative to siNT and error bars represent standard deviation from the mean; * $p \leq 0.05$ and ** $p \leq 0.01$ by student's t-test. D. Agarose gel analysis of RT-PCR products from RNA extracted from C2C12 myoblasts transfected in biological triplicate with siQk5-1 or siNT; increasing numbers of amplification cycles were run using otherwise identical conditions to amplify mRNA from pDup-Qk5i splicing reporter (top) and Gapdh (bottom); the relative mean band intensity from Dup-Qk5i reporter relative to Gapdh is shown below +/- standard deviation from the mean of three independent biological replicates (** $p < 0.01$; * $p < 0.05$) by student's t-test).

Figure S4 (supplemental to Figure 4): A. Schematic showing Qk5 RNA 3'end and primer sets used to measure total Qk5, unspliced Qk5, and read-through (non-polyadenylated) Qk5 measured in Fig 4C. B. Overview schematic of Qk5 3' intron and terminal coding sequence splicing reporter (pDup-Qk5i) experimental strategy (used in Fig 4D); top: UCSC Genome Browser screen showing (from top to bottom) RefSeq gene annotation, RBP Map, PanQKI CLIP peaks in HepG2 cells, PanQKI CLIP peaks in K562 cells, and conservation tracks. Dotted lines denote region cloned into pDup51 splicing reporter to make pDup-Qk5i. C. Representative western blot of protein extracted from C2C12 myoblasts co-transfected with pDup-Qk5i and either siNT or siQk5-3, probed with PanQk antibody and Gapdh antibody. D. UCSC Genome Browser screen shot of Qk5 3' end showing (from top to bottom) tracks for RefSeq, RBP Map, PanQKI CLIP peaks in HepG2 cells, PanQKI CLIP peaks in K562 cells, and QKI PAR-CLIP peak; inset below shows DNA encoding putative Qk binding motif ACTAAC (boxed, top, "wild type") and the substitution mutant sequence (bottom, "mutant" used in S4E). E. Representative western blots using whole cell extract from C2C12 myoblasts transfected with wild type renilla luciferase Qk5 3'UTR reporter and firefly luciferase control and either siNT, siQk, or siQk6/7 probed with PanQk and Gapdh antibodies. F. Measurement of renilla luciferase containing full length wild-type Qk5 3'UTR co-transfected with control firefly luciferase containing bovine growth hormone 3'UTR and either control siNT, siQk, or siQk6/7; renilla luciferase protein was normalized to firefly luciferase protein and fold change relative to control values are reported from three independent biological replicate experiments; error bars represent standard deviation from the mean. G. Measurement of renilla luciferase Qk5 3'UTR reporter protein normalized to transfection control firefly luciferase protein from whole cell extracts from C2C12 myoblasts transfected in biological triplicate with either full length wild type or full length mutant Qk5 3'UTR reporter; data displayed as fold change relative to wild-type Qk5 3'UTR reporter and error bars represent standard deviation from the mean.

Figure 5: Qk6 inhibits Qk5 translation but activates its own translation. A. Western blot of whole cell protein extracted from C2C12 myoblasts transfected with siNT, siQk5-1 and siQk6/7 probed with Qk5 or Gapdh antibody; Qk5 protein level is normalized to Gapdh protein and mean percentage protein abundance relative to siNT calculated from 3 independent biological replicates is shown at bottom, +/- standard deviation. B. RT-qPCR using RNA extracted from C2C12 myoblasts transfected in A. measuring Qk5 RNA normalized to Gapdh mRNA and shown as fold change relative to siNT; mean and standard deviation (represented by error bars) calculated from 3 independent biological replicates. C. Representative western blot of whole cell protein extracted from C2C12 myoblasts mock transfected, transfected with Myc-Qk5, and transfected with Myc-Qk6 plasmids simultaneously probed with antibodies to Qk6 (notation on right shows observed migration patterns of Myc-Qk6 and endogenous Qk6) and Gapdh; summary of mean protein and RNA abundance (determined by RT-qPCR) for endogenous Qk6 normalized to Gapdh and resulting translational efficiency relative to mock control +/- standard deviation is shown below in table format; * $p < 0.05$ by student's t-test. D. Measurement of renilla luciferase protein normalized to firefly luciferase protein from protein extracted from C2C12 myoblasts transfected with renilla luciferase Qk6 3'UTR and firefly luciferase control reporters and either tdTomato or Myc-Qk6 plasmids; data collected from 3 biological replicate experiments are shown as fold change relative to tdTomato control and error bars represent standard deviation from the mean.

Figure S5 (supplemental to Fig 5): A. Representative western blot of C2C12 myoblasts mock transfected, transfected with Myc-Qk5, or Myc-Qk6 simultaneously probed with Qk5 (top) and Gapdh (bottom) antibodies. B. Western blots of whole cell protein lysates from C2C12 myoblasts co-transfected with renilla luciferase-Qk6 3'UTR reporter and firefly luciferase transfection control reporter plus either tdTomato control plasmid or Myc-Qk6 plasmid simultaneously probed with antibodies to DsRed2 (reacts with tdTomato), Qk6 and Gapdh.

Figure 6: Qk cross-isoform regulation is conserved in rat C6 glioma cells. A. Western blots were simultaneously probed with antibodies to Qk5 and PanQk, Qk6 and PanQk, or Qk7 and PanQk (see Fig S6A) and infrared intensity values for each isoform were normalized to PanQk and used to determine mean percentage of each protein isoform relative to total (PanQk) in whole cell protein extracts from C2C12 myoblasts, rat C6 glioma cells, rat CG4 oligodendrocyte precursor cells, mouse optic nerve tissue, and mouse cerebellum sampled in biological triplicate. B. Representative western blot of whole cell protein extracts from rat C6 glioma cells transfected with siNT, siQk5-1, and siQk6/7 simultaneously probed with Qk5 and Gapdh antibodies; quantitation of mean infrared signal for Qk5 normalized to Gapdh from three biological replicates and reported below as percentage protein abundance relative to siNT and +/- standard deviation. C. RT-qPCR of RNA extracted from biological triplicate cultures of rat C6 glioma cells described in B measuring Qk5 RNA normalized to Mapk3 mRNA and displayed as fold change relative to siNT +/- standard deviation (* $p < 0.05$). D. Representative western blot of whole cell protein extracts from rat C6 glioma cells described in B but probed with Qk6 and Gapdh antibodies; quantitation of mean infrared signal for Qk6 relative to Gapdh reported below as percentage protein abundance relative to siNT and +/- standard deviation of the mean calculated from 3 independent biological replicates. E. RT-qPCR of RNA extracted from rat C6 glioma cells described in B measuring Qk6/7 RNA normalized to Mapk3 mRNA and displayed as fold change relative to siNT +/- standard deviation (* $p < 0.05$).

Figure S6 (Supplementary to Fig 6): A. Representative western blots of whole cell protein extracts from C2C12 myoblasts, rat C6 glioma cells, rat CG4 oligodendrocyte precursor cells, mouse optic nerve tissue, and mouse cerebellum tissue probed with Qk5 in red channel and PanQk in green channel (top), Qk6 in red channel and PanQk in green channel (middle), and Qk7 in red channel and PanQk in green channel (bottom); signal intensities used to calculate data in Fig 6A. B. Representative western blot using whole cell protein extracts from rat C6 glioma cells transfected with siNT, siQk5-1, and siQk6/7 simultaneously probed with antibodies to Qk7 and Gapdh; Qk7 signal intensity normalized to Gapdh and reported as mean percentage protein abundance relative to siNT +/- standard deviation of the mean from 3 independent biological replicates.

Figure 7: Models of Qk autogenous regulation. A. Quantitative rheostat model: various relative levels of Qk protein isoforms are observed in different cell/tissue types such as Qk5 high/Qk67 low in C2C12 cells, medium Qk5/medium Qk67 in rat C6 glioma cells, and high Qk67/low Qk5 in adult mouse optic nerve and cerebellum tissues. These different relative protein levels support the observed auto- and cross-isoform regulatory interactions defined in this study, albeit by imposing greater influence (thicker lines) on specific processing steps when their relative concentration is higher (larger font) than in other cell/tissue types. Arrows denote positive regulation while lines ending in perpendicular line denote negative regulation. B. Hierarchical model: the *Qk* gene transcribes a single pre-mRNA which is processed to make mature Qk mRNA isoforms which are then exported from the nucleus and translated into Qk5 and Qk6 proteins. The NLS unique to the Qk5 C-terminus mediates nuclear import, thus more Qk5 protein is observed in the nucleus. Here Qk5 promotes nuclear accumulation of Qk pre-mRNA and formation of Qk5 mRNA through a splicing based mechanism. Accumulation of Qk5 protein negatively feeds back to reduce its own levels, while it also positively feeds back to promote accumulation of Qk6 mRNA. Qk6 protein is predominantly localized in the cytoplasm and negatively regulates the translation of Qk5, and positively regulates its own translation. Dotted lines represent regulatory interactions, while solid lines represent spatial and temporal flow of genetic information.

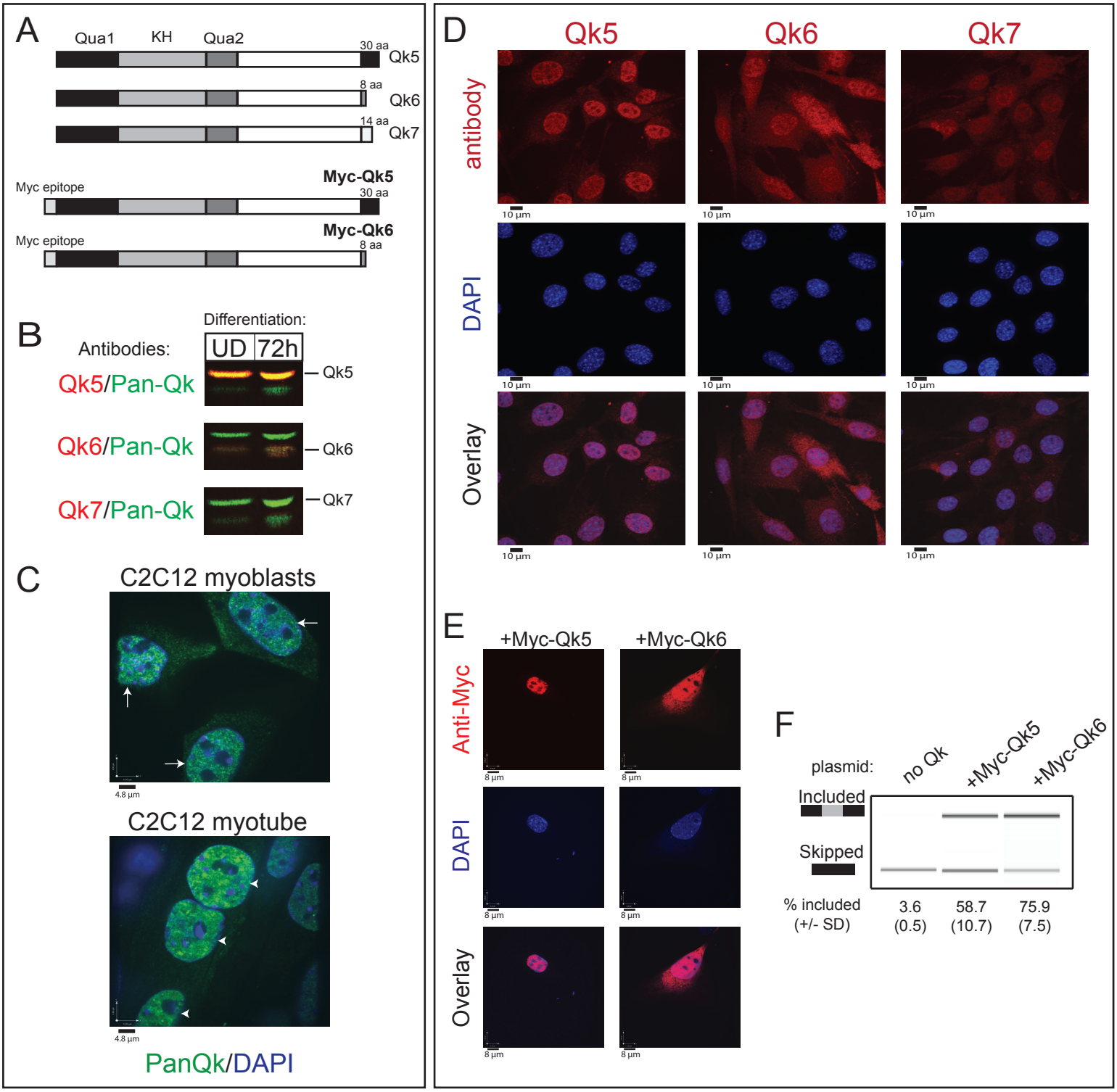

Figure 2

Fagg_Fig2

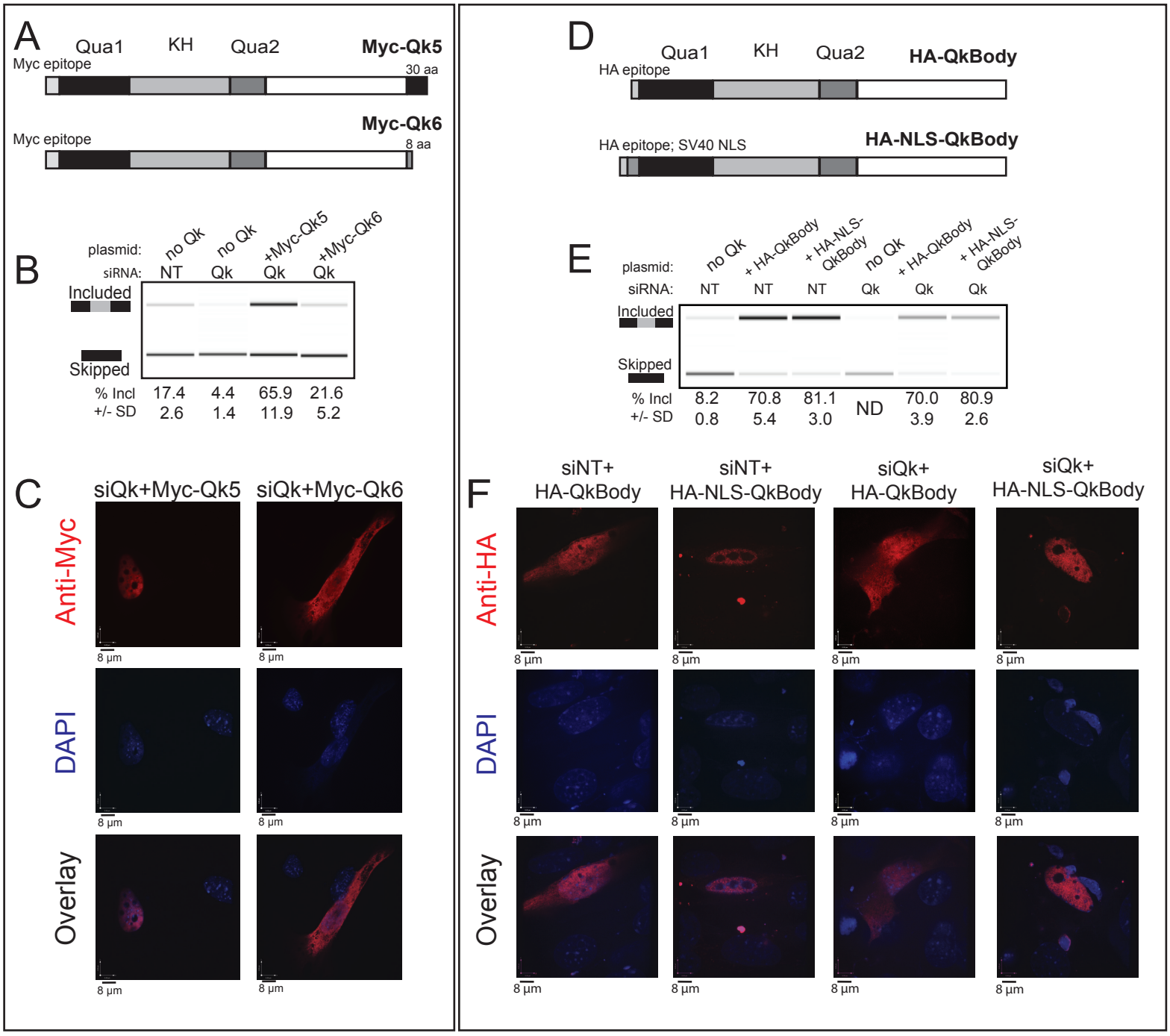

Figure 3

Fagg_Fig3

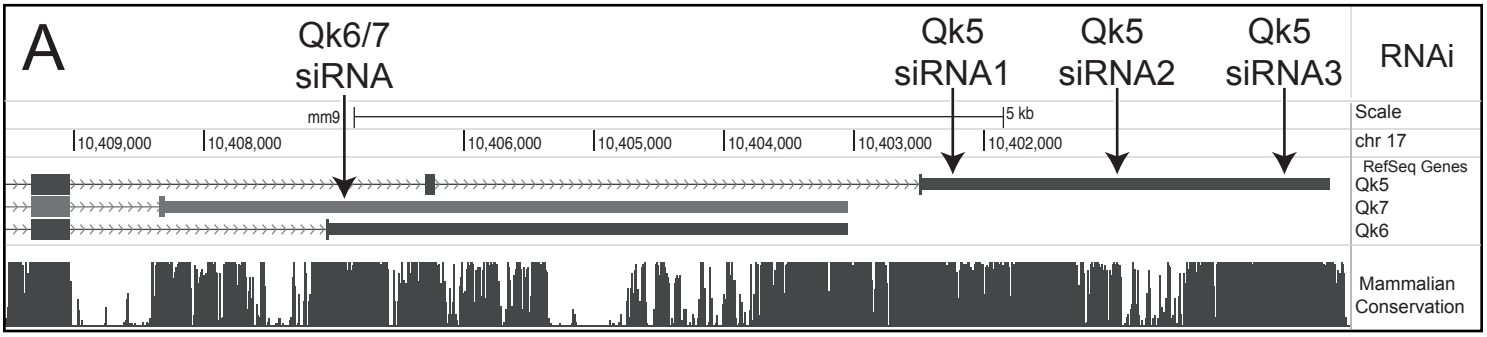

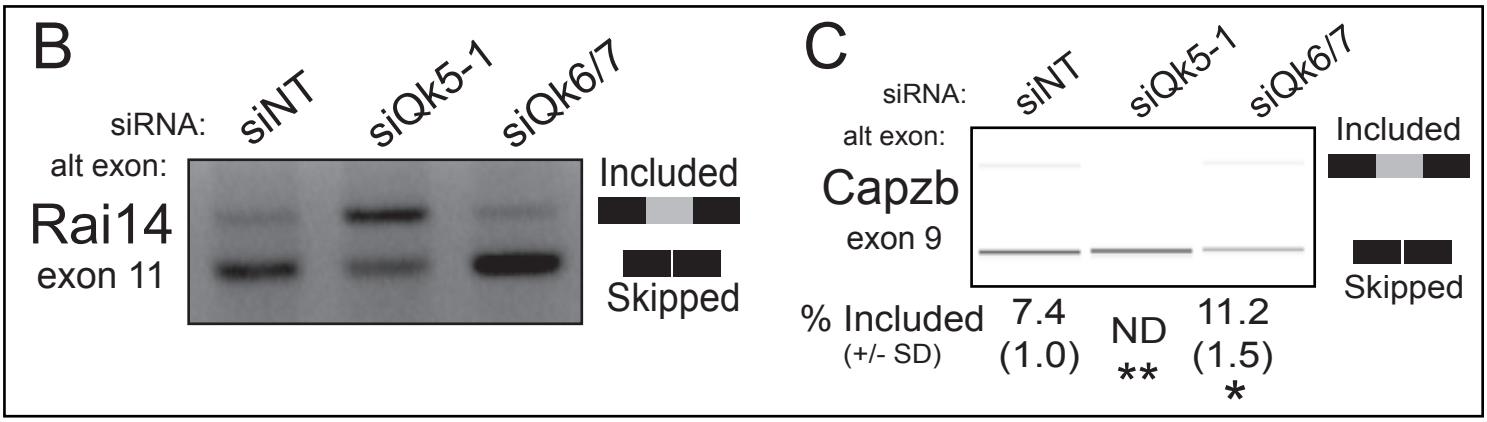

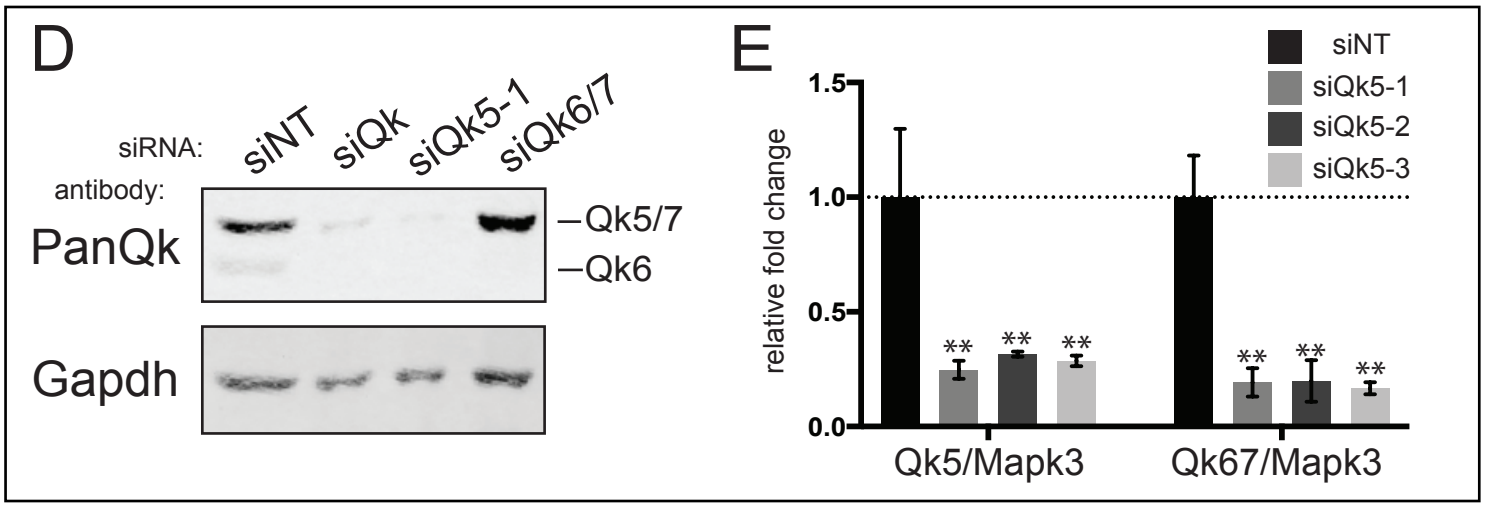

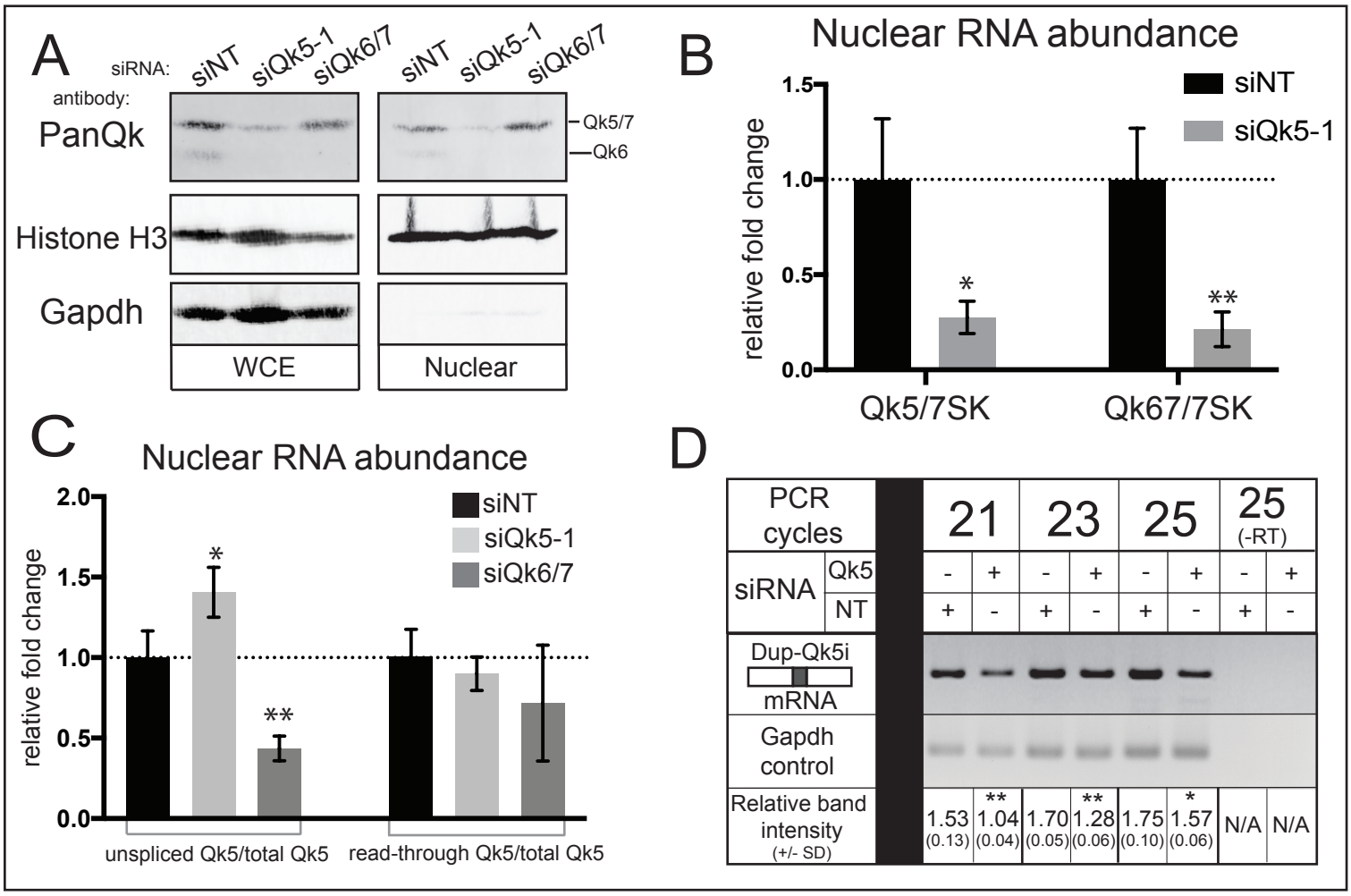

Figure 5

Fagg_Fig5

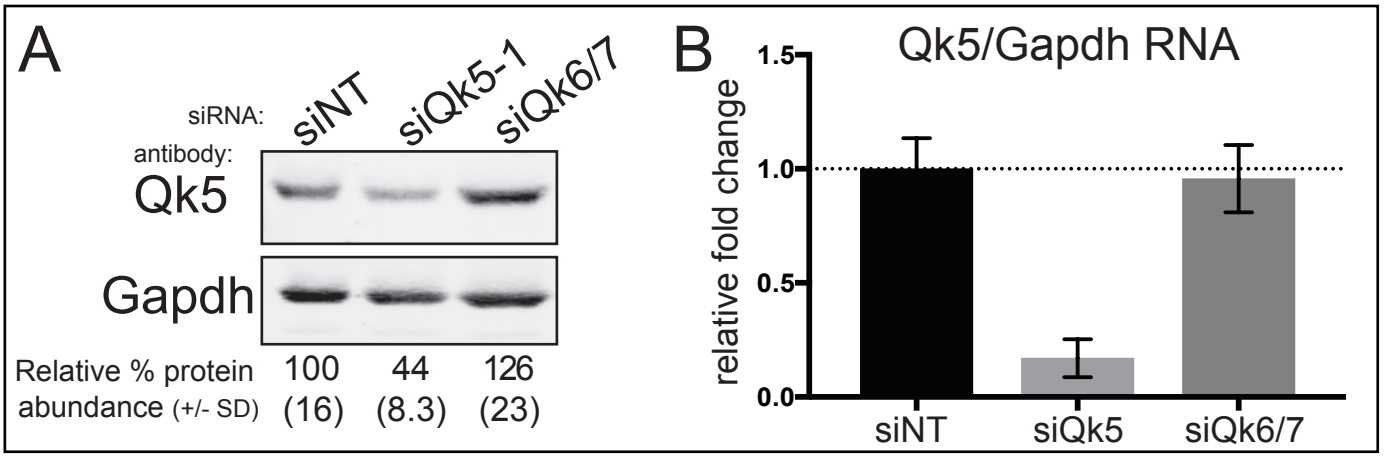

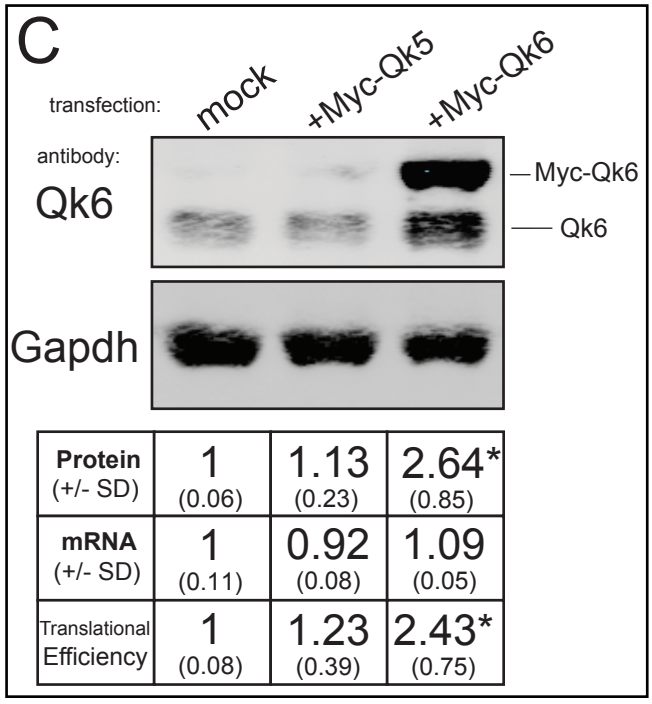

Protein (+/- SD)	1 (0.06)	1.13 (0.23)	2.64* (0.85)
mRNA (+/- SD)	1 (0.11)	0.92 (0.08)	1.09 (0.05)
Translational Efficiency	1 (0.08)	1.23 (0.39)	2.43* (0.75)

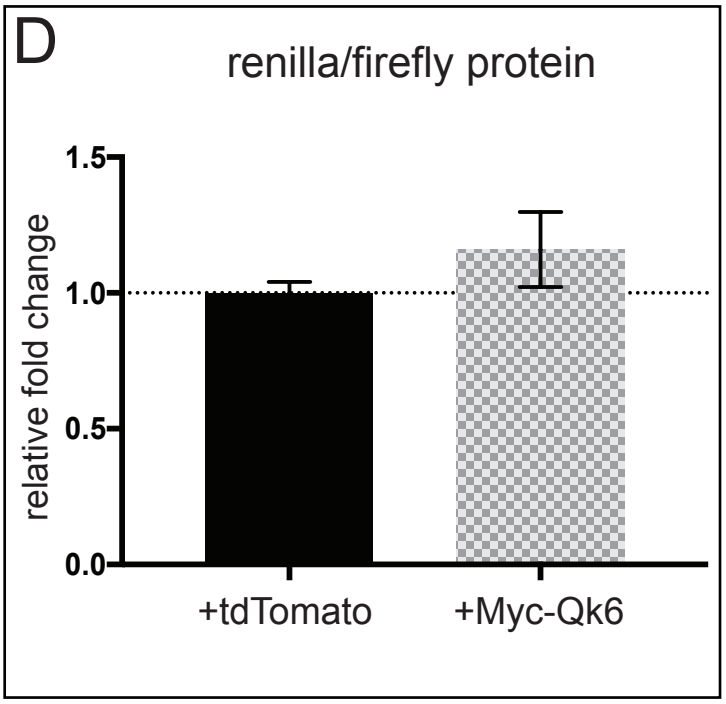

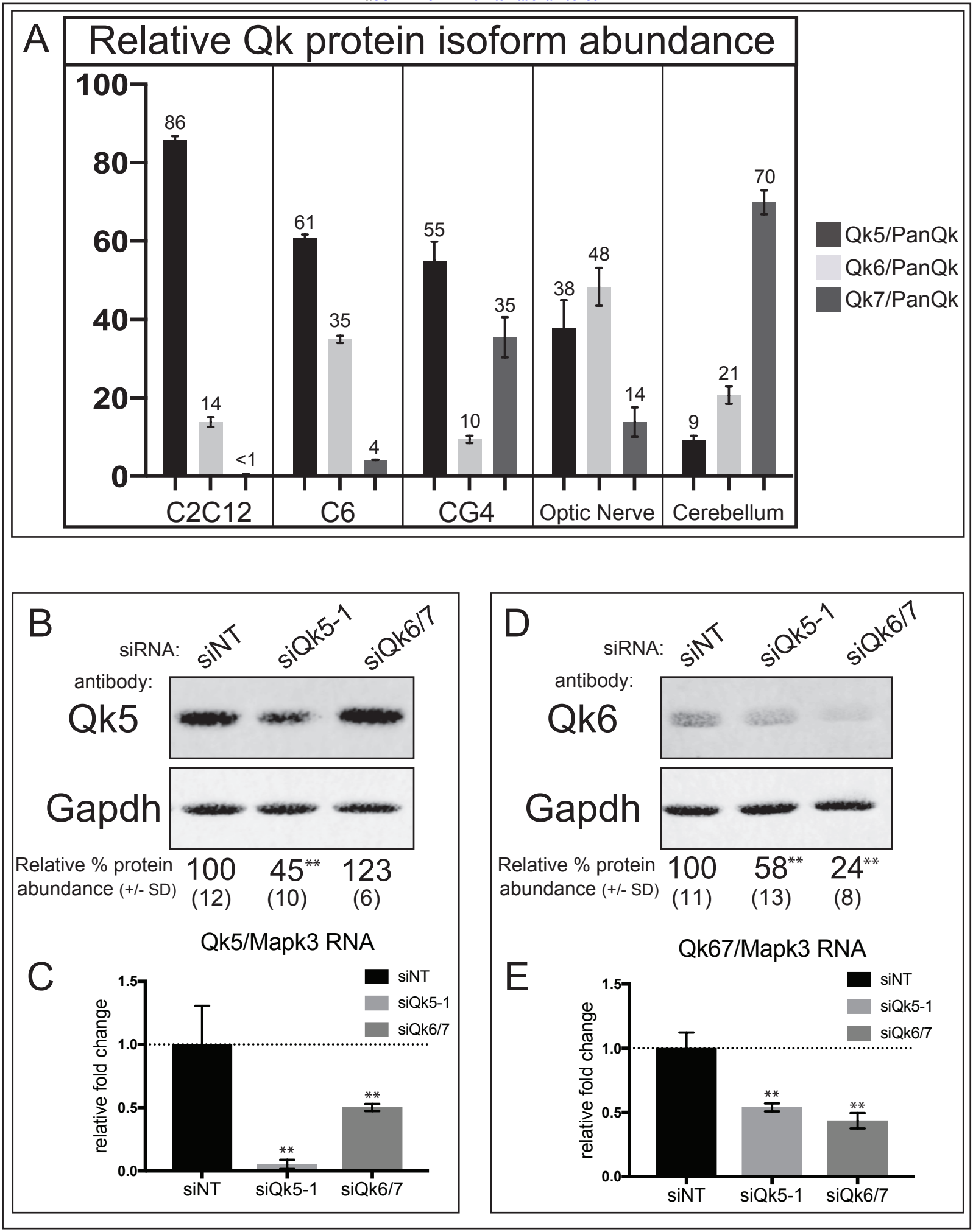

Figure 7

Fagg_Fig7